Materials Today Physics 44 (2024) 101441

Contents lists available at ScienceDirect

Materials Today Physics

journal homepage: www.journals.elsevier.com/materials-today-physics

Towards local tracking of solvated metal ions at solid-liquid interfaces

William Trewby [a,b,c], Mahdi Tavakol [a], Ygor Morais Jaques [d,e,f], Kislon Voïtchovsky [a,*]

[a] Physics Department, Durham University, Durham, DH1 3LE, UK
[b] Department of Physics and Astronomy, University College London, London, WC1E 6BT, UK
[c] London Centre for Nanotechnology, University College London, London, WC1H 0AH, UK
[d] Department of Applied Physics, Aalto University, Espoo, Finland
[e] Centre of Excellence in Life-Inspired Hybrid Materials (LIBER), Aalto University, Espoo, Finland
[f] Department of Chemistry and Materials Science, Aalto University, Espoo, Finland

ARTICLE INFO

Keywords:
Solvated ions
Solid-liquid interfaces
Diffusion
Aqueous solutions
Hydration interactions
Atomic force microscopy
X-ray spectroscopy
Non-linear spectroscopy
Molecular dynamics
Computer simulations
Stern layer

ABSTRACT

The dynamics of individual solvated ions near solid surfaces is the driving force behind numerous interfacial processes, from electrochemical reactions to charge storage, mineral growth, biosignalling and bioenergetics. The precise system behaviour is delicately dependent on the atomistic and molecular details of the interface and remains difficult to capture with generalisable, analytical models. Reported dynamics can vary by orders of magnitude depending on microscopic details of the solvent, ions and/or surface chemistry. Experimentally, tracking single solvated ions as they move at or along interfaces remains highly challenging. This is, to some extent, offset by simulations that can provide precise atomistic insights, but usually over limited timescales. The aim of this review is to provide an overview of this highly interdisciplinary field, its achievements and remaining challenges, reviewing both experimental and computational results. Starting from the well accepted continuum description of dissolved ions at solid-liquid interfaces, we outline the challenges of deriving local information, illustrating the discussion with a range of selected studies. We explore the challenges associated with simultaneously achieving the spatial and temporal resolution needed to gain meaningful, yet contextual insights of single ions' dynamics. Based on the current studies, we anticipate the future developments in the field, outlining remaining challenges and opportunities.

1. Introduction and scope of the review

Boundaries between electrolytic solutions and charged solids are an almost universal feature of the natural world, and many dynamic processes depend on them, including geochemical interactions between oceans and the earth's crust [1,2], the use of ions for bioenergy [3–5], sensing and signalling [6–8], and the stability of plant and food systems [9]. In technology, a better understanding of these solid-electrolyte interfaces is crucial for advances in colloidal stability [10–12], water purification [13,14] and electrochemical processes [15,16]. Currently, their importance is further underlined by the need for clean batteries, fuel cells and supercapacitors that will power the next generation of electrical devices [17–23].

Conceptually, the interface between an electrolyte and the surface of a solid is an infinitely thin region lying at the boundary between the two media. In reality, these interfaces have a finite thickness, extending a few molecular diameters (typically up to 2 nm) into the electrolyte solution [24–29]. In this region, solvent molecules and ions tend to be less mobile and more organised than in the bulk electrolyte [30–35]. This is due to a combination of direct interactions between the solvent molecules and ions with the surface of the solid, and a loss of configurational entropy [36–39]. As such, solid-electrolyte interfaces have unique properties that often differ significantly from the bulk fluid phase. One key aspect of these interfacial systems is their dynamics. Electrostatic interactions and solvent-mediated effects are in constant competition with the charges' thermal motion [33,37], which can generate diverse static [29,40–42] or time-dependent structures [43–45]. This occurs, for example during capacitive charging [16,46] or crystal formation, growth and dissolution [47–52].

In order to develop a holistic picture of solid-electrolyte interfaces it is necessary to take into account electrostatic interactions, but also the short-ranged nature of specific solvent interactions and, where relevant, the atomic-level details responsible for non-linear and cooperative molecular effects [2,23,44,53–60]. There is hence a pressing need to

---

* Corresponding author.
E-mail address: kislon.voitchovsky@durham.ac.uk (K. Voïtchovsky).

https://doi.org/10.1016/j.mtphys.2024.101441
Received 15 January 2024; Received in revised form 11 April 2024; Accepted 14 April 2024

develop methods, both experimentally and *in silico*, that can track the dynamics of dissolved ions and charges at the interface with solids on a "local" scale – that is, being able to account for single-ion effects while still capturing contextual effects and emergent cooperative behaviour. For example, effects such as ion-ion correlations and overscreening are often seen as the root of discrepancies between theory and experiments [61,62], but until recently it has not been possible to investigate or confirm these effects directly at the atomic-level where they occur [55]. Advances in spectroscopic techniques, scanning probe microscopies and molecular dynamics simulations have made possible the tracking of individual charges at interfaces and thus revitalised scientific interest in the field [30,40,63–65].

This review aims to survey the various historic and current frameworks that have been used to describe electrolytes at interfaces, leading to the state-of-the-art experiments and modelling that reveal the structure and dynamics of individual metal ions in a solvent. We begin in section 2 by discussing the theories which model the solid-liquid interface as being (at least in part) continuous. These are enormously successful at the micro- and mesoscale and for "reasonable" surface charge densities or ionic strength. However, it does not require particularly extreme conditions for such approaches to break down, and we will highlight the areas where more insight is needed. Section 3 elaborates on the various time and length-scales that emerge from theoretical treatments of ions at interfaces, and to what extent we can probe these both experimentally and computationally. We then inspect key examples where non-linear interfacial ion dynamics produce anomalous results that cannot easily be fitted into traditional frameworks. Section 4 presents our current best-picture of solid-electrolyte interfaces at rest from experiments and simulations. We emphasise the inherent difficulties in conducting and interpreting these experiments, despite the simplification of disregarding time-dependent phenomena. Computational methods are a crucial complement to experimental studies, providing true atomistic precision and insight into these interfacial systems. However, they are not without their own limitations, and we emphasise the necessity of a holistic approach when exploring the interfacial nanoscale behaviour of electrolytes. Section 5 reviews the latest advances in the field towards tracking individual ions at solid-electrolyte interfaces while simultaneously obtaining the contextual information necessary to interpret the observations. The section focuses primarily on experimental efforts with scanning probe microscopies and theoretical computer simulations. The final section summarises the perceived key developmental challenges in the field. Based on this, future directions for research and applications are proposed.

The review focus on interfaces where the electrolyte is composed of ions dissolved into a solvent. Interfaces involving pure solvents or solvent-free electrolytes (ionic liquids) are addressed in other reviews [66–68].

2. Continuum-based descriptions of the interface

Modelling solid-electrolyte interfaces is a century-old problem, with the first theoretical models emerging from the work of Helmholtz [69], Gouy [70] and Chapman [71]. These models rely on a few key simplifications: ions or charged molecules are considered as point charges in a continuous solvent described solely by its unchanging dielectric constant. Such continuum assumptions make a theoretical description of the interface considerably easier and remove the need to model local molecular interactions explicitly. Continuum-based models of solid-electrolyte interfaces have proved very successful, often down to the nanometre scale. They are still largely used today both as a reference and for making predictions in systems where molecular details can be ignored. The topic has been extensively covered by textbooks [37,72,73] and reviews [2,74], here we only focus on the concepts that are relevant for this review.

2.1. The electrical double layer and Poisson-Nernst-Planck model

The best-known theoretical framing of electrolyte-solid interactions is arguably that of the electrical double layer (EDL), which bridges two conceptually distinct portions of the interface. In this framework initially developed well over a century ago [69–71,75,76], the first layer is associated with the solid and is composed of charges present on the surface as it is immersed into a liquid (Fig. 1(a)). In the case of an electrical insulator, such as an oxide, these charges develop naturally. They are chemically bound to the solid and usually have an entropic origin, whereby some surface groups dissociate in solution, resulting in a net surface charge. A similar effect can be achieved by surface design

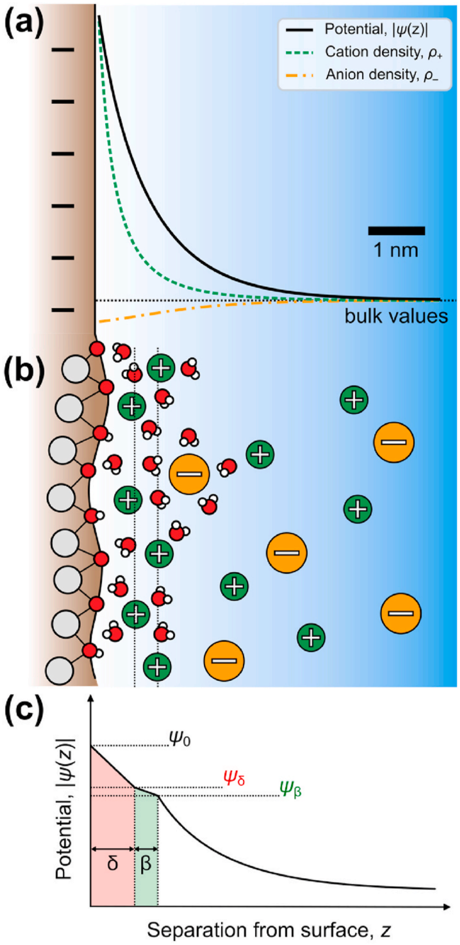

Fig. 1. | The varying complexity of models for solid-liquid interfaces. (a) An idealised interface between a uniformly charged, flat solid and a continuous electrolyte. This system is well-described by equations (1)–(3), allowing the calculation of the (absolute) electric potential and its z-dependence, $|\psi(z)|$, as well as the cation and anion density, $\rho_\pm$. Here, for a bulk monovalent ion concentration of $\rho_\infty = 100$ mM and a surface charge density of $\sigma = -0.39\ e\,\mathrm{nm}^{-1}$, the Debye length, $\lambda_D = 0.96$ nm, and the bulk values of $\rho_\pm$ and $\psi(z)$ are already reached ~5 nm away from the solid. A more realistic model of the interface, depicted approximately to scale in (b), must accommodate variation in topography and surface chemistry, as well as the finite sizes of solvent molecules (here water) and ions, and their specific adsorption to the solid. One way to extend the Poisson-Boltzmann formalism is to allow ions to adsorb directly and indirectly (*via* solvent molecules) in two planes of thickness δ and β (dashed lines). These each have distinct dielectric properties that result in linear decreases in the potential (c), which is electrically equivalent to the layers acting as planar capacitors in series at the interface. These models are more realistic, but fundamentally remain 1D depictions of the system, with no truly local information. Note that *absolute* potentials are presented in (a) and (c): for the depicted systems, we would have $\psi < 0$.

and modification [77,78] or imposing of an electrostatic potential with respect to the electrolyte in the case of a conducting solid [79]. In all cases, the solid's surface is assumed to be homogenous and described by an effective potential, ψ_0, and charge density σ. This constitutes the first layer. By simple electrostatics, counterions in the liquid will accumulate adjacent to the first layer to compensate this electric field. However, these counterions are mobile, and the electrostatic interactions are coupled with thermal fluctuations that encourage the solutes to be more evenly distributed within the liquid. This forms the second layer of the EDL – the so-called diffuse layer. In the diffuse layer, the density of the ions, $\rho(z)$, at any given distance, z, from the surface is related to the electrostatic potential $\psi(z)$ at that distance through the one-dimensional Poisson equation:

$$\frac{d^2\psi(z)}{dz^2} = -\frac{\alpha e}{\varepsilon_r \varepsilon_0}\rho(z), \tag{1}$$

where α is the valence of the ionic species considered and e is the elementary charge. The vacuum permittivity and relative permittivity of the electrolyte are given by ε_0 and ε_r respectively, emphasising the fact that this theory takes the solvent as continuous and ignores any specific interactions with dissolved ions. The expected balance between electrostatic and thermal energy for the ions in the diffuse layer is captured by the Boltzmann distribution, so that the density $\rho(z)$ of ions obeys $\rho(z) = \rho_\infty \exp(-\alpha e \psi(z)/k_B T)$ where ρ_∞ is the concentration of ions in bulk electrolyte, k_B is Boltzmann's constant and T is the absolute temperature. This assumption leads to the well-known Poisson-Boltzmann equation:

$$\frac{d^2\psi(z)}{dz^2} = -\frac{\alpha e}{\varepsilon_r \varepsilon_0}\rho_\infty \exp\left(-\frac{\alpha e \psi(z)}{k_B T}\right). \tag{2}$$

Assuming a planar interface and a small surface potential (typically $\psi_0 < 25$ mV), the equation can be linearised (in the Debye-Hückel approximation [80]) and solved analytically. For symmetric electrolytes, it yields the following solution (see e.g. Ref. [37]):

$$\psi(z) \approx \psi_0 \exp\left(-\frac{z}{\lambda_D}\right); \quad \lambda_D = \sqrt{\sum_i \frac{\varepsilon_r \varepsilon_0 k_B T}{\rho_{\infty,i}(\alpha_i e)^2}}. \tag{3}$$

The summation is over each ionic species, i, present in the electrolyte. Equation (3) demonstrates a straightforward exponential decay into the bulk fluid, with the characteristic length scale of the decay given by a constant known as the Debye length, λ_D, which varies with the ionic valency and bulk concentration. The Debye length provides a useful estimate for the size of the diffuse layer and quantifies the extent to which the interface perturbs the bulk electrolyte, as illustrated in Fig. 1 (a) – this typically ranges from hundreds of nanometres in dilute solutions to just Ångströms at moderate ionic strengths. Conceptually, the diffuse ionic layer is seen as spatially homogenous at a given distance from the surface, and its total ion content can be calculated by combining equation (3) with the Boltzmann distribution. In fact, the assumption of electroneutrality requires that the solid's surface charge, σ, is exactly balanced by the charges present in the double layer, thus imposing a direct relationship between σ and ψ_0, known as the Grahame equation [76]. In this picture, the EDL then forms a uniform capacitor of thickness $\sim \lambda_D$ with plate charges of $\pm\sigma$.

To partly account for the finite spatial extent of the adsorbed counterions, and the supposition that adsorbed ions are less mobile than in the diffuse layer (Fig. 1(b)), a semi-empirical approach assumes there exists a strongly adsorbed counterion layer at the surface of the solid. This region is often referred to as the Stern layer and is seen as an immobile region of the same width, δ, as an ion at the surface. Practically, this view can be incorporated into the Poisson-Boltzmann formalism by modelling the Stern layer as a homogenous planar capacitor with a distinct dielectric constant $\varepsilon_\delta < \varepsilon_r$ to reflect the reduced solvent density in the layer. This induces a linear drop in potential $\psi_\delta = \sigma\delta/\varepsilon_0\varepsilon_\delta$ through the layer, followed by the exponential decay predicted by the Poisson-Boltzmann equation (Fig. 1(c)). Further refinements allow ions to adsorb indirectly to the solid *via* their solvation shell, hence inducing a larger separation, $\delta' = \delta + \beta$, and resulting in two capacitive layers at the interface (Fig. 1(c)). In this context, the ionic structures are usually referred to as the inner and outer Helmholtz layers, reflecting ions adsorbed directly (known as inner-shell coordination) or indirectly (outer-shell coordination), as depicted schematically in Fig. 1(b).

The Stern and diffuse layers combine in the EDL to give a conceptually useful model that can be applied to a range of macroscopic experiments [10–12,72,81–83] and acts as a reference point for any attempt to describe ion organisation at interfaces or in the presence of an applied electric field [74,84]. However, the picture is a fundamentally static one that implicitly assumes thermodynamic equilibrium. Further developments are needed to describe time-dependent process and capture the response of ions to changes in the interface geometry or applied electric fields. A common way forward is the Poisson-Nernst-Planck (PNP) formalism [85] which couples the spatial behaviour of equation (2) to the dynamic, diffusive nature of the dissolved ions:

$$\frac{\partial \rho(z,t)}{\partial t} + \nabla \bullet \boldsymbol{J} = 0, \tag{4}$$

where $\rho(z,t)$ is now the concentration of an ionic species at a given point in space and time, and $\boldsymbol{J}$ represents its flux. The PNP approach offers a versatile mean for studying ionic dynamics and can be straightforwardly modified to account for large applied potentials [86], steric interactions between ions [59] and more complex geometries [81,87]. These alterations render the models more capable of describing realistic time-dependent processes at solid-electrolyte interfaces and can be computationally advantageous to molecular dynamics simulations [88, 89].

2.2. Theoretical length scales and time scales

Continuum theories predict different characteristic length and time scales that offer clues about which effects dominate for a given interface, depending on the scale considered. These characteristic scales aim to capture the *collective* behaviour of ions at interfaces. Arguably, the best-known length scale is the Debye length, λ_D, as already introduced in equation (3). Although it relies on bulk properties of the solvent and ignores complexities of the surface, its enduring appeal and continued use reflect its empirical success.

Another key distance in the context of ionic correlations is the Bjerrum length, l_B, defined as the separation between two point-charges at which the Coulomb energy balances the thermal energy:

$$l_B = \frac{e^2}{4\pi\varepsilon_0\varepsilon_r k_B T}. \tag{5}$$

In pure water and a room temperature, $l_B \sim 0.7$ nm for monovalent ions. The direct application of this concept to real systems is limited by the uncertainty of the solvent's dielectric response: the decrease in ε_r near surfaces [31] or strongly charged ions could result in a dilated length of up to $l_B \sim 10$ nm [59].

Temporally, if the ions' bulk diffusion coefficient, D, is known, λ_D can further be used to define two timescales associated with ionic motion. The first is known as the Debye time, τ_D, defined as [12,85]:

$$\tau_D = \frac{\lambda_D^2}{D}. \tag{6}$$

This quantity describes the time required for an ion to diffuse over the length of λ_D, and provides an indication of how quickly the diffuse layer can respond to an electric perturbation. For systems with an applied overpotential (such as immersed parallel-plate electrodes), this implies that any time-varying fields of frequency $\nu > \tau_D^{-1}$ will not allow the interface to be electrically relaxed [47,90,91] – i.e. dissolved ions can no longer rearrange in response to the oscillating field. For monovalent metal ions ($D \sim 10^{-9}$ m^2/s) with a concentration c in aqueous solutions, τ_D typically ranges from sub-nanosecond ($c = 100$ mM) to tens of nanoseconds at lower ionic concentrations. This gives a range of MHz to GHz for non-linear electrokinetic behaviours to emerge, depending on c.

A second, closely related timescale can be used to better incorporate the geometry of a given setup (e.g. the distance between electrodes). For a system with characteristic length, L, and assuming the EDL behaves as an ideal capacitor (see section 2.1), the time scale associated with the charging of the capacitor by dissolved ions, τ_{RC}, is given by Refs. [47, 85]:

$$\tau_{RC} = \frac{\lambda_D L}{D}, \tag{7}$$

where τ_{RC} is known of the *RC* timescale, by analogy to electric resistor-capacitor (RC) systems. For many macroscopic systems where $L \gg \lambda_D$, the RC charging time is much larger than the Debye time. This is not necessarily true in nanoscale systems where interfacial effects and diffusion constraints can dominate [47,90]. Generally, operating at fast timescales (high electrical frequencies) and nanometre spatial scales require taking into account the different dynamics at play explicitly. This can often be modelled using PNP, for example when optimising sensing with nano-electrodes in electrical impedance spectroscopy [92].

2.3. *The breakdown of continuum models*

Continuum descriptions like the Poisson-Boltzmann and PNP models are accurate and flexible enough to allow their application in countless electrostatic and electrokinetic systems [82,93–96]. However, their success is almost always contingent on intensive fitting routines aimed at determining “effective” continuum parameters and ensuring self-consistency. For example, the dielectric constant of a Stern layer of ions is not known *a priori*, and an effective value is needed to describe an average effect across the whole interface. Depending on the system considered, fitting experimental results with the Poisson-Boltzmann-Stern framework can return an unphysically wide Stern layer [97] (position of the “slip plane”, β in Fig. 1(c)). Additionally, a direct link between the charge density and potential of any given surface (such as the Grahame equation) often requires self-consistent fitting of underdetermined datasets, with results varying dramatically depending on the experimental technique being used [98,99]. Such discrepancies can often be attributed to the assumption that the system is at equilibrium. The inconstant validity of this assumption is illustrated by measurements of colloidal interactions through “static” ionic distributions that are captured well by equation (2), often conducted through “dynamic” electrophoretic measurements [72] that depend sensitively on the coupling between fluid and ionic motion, as well as specific adsorption at the interface.

Aside from these practical issues, more fundamental problems become apparent when extrapolating continuum models to the nanoscale. A key sticking point is the assumption that ions are point-like charges immersed in a continuous, isotropic, dielectric solvent. While generally valid for dilute solutions and at larger (>5–100 nm) distances from a surface with a low charge density, it still requires ionic interactions to be solely electrostatic, an assumption that does not always stand up to scrutiny [100,101]. Additionally, ions can exhibit some spatial correlation near and within the Stern layer [30,44,102–105], with the specific position of a given ion influencing the location and behaviour of its neighbours (Fig. 2). Such effects are not easily captured by continuum models.

Similarly, the timescales derived from the Poisson-Boltzmann framework are conceptually useful to estimate the kinetics associated with the EDL, but they also suffer from their reliance on bulk ionic diffusivities and the assumption of a continuous solvent [12]. They can thus break down or require extension in non-ideal conditions such as large applied potentials [86]. Recent work exploring the forces generated by electrolytes under ac fields – that is, the dynamic response of ions to varying forcing frequencies – has also called into question the validity of such simplified timescales. These have illustrated the extra insight required to understand the sign of the force [106] and the role of specific geometries and cation/anion diffusivity [90,107].

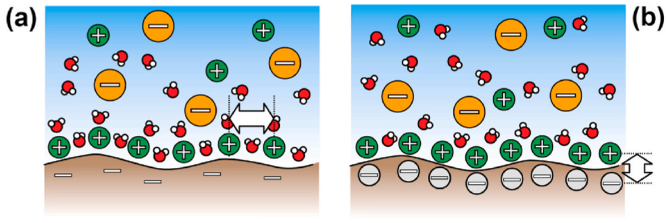

Fig. 2. | Example of ion-ion correlations at solid-electrolyte interfaces. Lateral correlations (a) occur when adsorbing ions interact with each other in the plane other parallel to the interface, typically within the Stern layer. The interaction can be direct (electrostatics) [102–105 102–105 102–105] or indirect (e.g. involving solvent molecules, as represented here) [30,44]. Direct electrostatic coupling can be predicted by the balance of electrostatic and thermal energies (coupling parameter [104,105] related to the Bjerrum length). It is normally repulsive and most common among multivalent ions. In contrast, solvent-mediated correlations can be effectively attractive between ions and occur with monovalent species. Transverse correlations (b) occur perpendicular to the interface, typically where counterions are directly adsorbed onto localised charges of the surface of the solid. This order can further propagate into the liquid, creating ionic layers. The figure has been inspired by Faraudo and Travesset [104] where a more thorough and quantitative description of correlation effects is presented, including the interplay between lateral and transverse correlations and other types of correlations such as complexation.

Generally, most models conceived within a continuum framework struggle to capture meaningful, molecular-level details of the interface [108] even in relatively straightforward conditions. For example, at a monovalent ionic strength of 150 mM, the average separation between charges in bulk will be ~1.8 nm, but this distance will quickly drop below a nanometre at a charged interface. Considering a typical hydrated metal ion with a diameter of 0.4–0.7 nm [109], it is obvious that non-Coulombic forces such as steric or molecular interactions can dominate over ionic interactions [110–112]. These effects are usually system- or ion-specific and cannot easily be accommodated even by modified PNP models. The dominance of these non-classical interactions is the norm in biological systems [36,102,113–116], which tend to exist in “non-ideal” ionic environments that violate continuum assumptions – a fact that nature regularly takes advantage of [6]. Similarly, short-ranged interactions between ions, waters and the surface can play a significant role in determining interfacial structure and dynamics, dominating electrostatics in some cases (more in sections 4 and 5).

Arguably, the most important limitation of mean-field models is their assumption of a homogenous interfacial plane. While models can be used to calculate effective charge densities for equivalent “smeared-out” systems, there is no way of encoding or predicting the lateral ionic correlations (Fig. 2), atomic defects or surface charge regulation that have been observed experimentally [30,44,64,117–120]. At the nanoscale, it is often precisely details of the surface heterogeneity that dominates interfacial processes, for example in crystal growth and dissolution [48,50,51], heterogenous catalysis [15], or the emergence of novel interfacial iontronics [121–124]. Further, even at moderate separations, the forces generated by dynamic rearrangement of concentrated electrolyte solutions often cannot be explained by diffusive and continuum descriptions of the fluid, requiring more complexity than a straightforward dielectric [90,106]. With recent results showing that short-ranged hydration interactions can be fully de-coupled from electrostatic interactions [125], the use of continuum models to capture the motion of single ions at solid-liquid interfaces is necessarily limited.

3. The question of scale: global vs local observations

Section 2 highlights the beauty and predictive power of continuum descriptions of the solid-electrolyte interface, but also contrasts the simple length- and timescales derived with the molecular complexity of realistic interfaces. To access and quantify this complexity, measurements are needed on a broad range of real-world systems. The aim of this section is to briefly review some of the main experimental (section 3.1) and computational (section 3.2) approaches currently taken, discussing in each case their strengths and limitations, as well as precisely the type and scale of information that can be derived (Fig. 3). Many modern techniques can achieve sub-molecular precision, but the associated temporal sensitivity and the level of averaging required varies. Generally, a compromise needs to be found between spatial resolution, temporal resolution, and the number of molecules interrogated (Fig. 3). Here, we aim to draw together these often-disparate representations and highlight their shared strengths as well as the global picture of solid-electrolyte interfaces that emerges. Finally, section 3.3 highlights some of the current gaps and opportunities with existing techniques in the context of local probing of ions' dynamics at a solid-electrolyte interface. Based on existing techniques and theory, the discussion also aims to address questions such as what constitutes "local" information? What are the associated spatial and temporal scales? How are these scales coupled? What is the boundary between equilibrium behaviour and dynamics on the relevant scales?

3.1. Experimental techniques

Experimental techniques have the advantage of being more model-agnostic in their conclusions when compared to theoretical predictions. However, interfacial ions, as well as the systems they interact with, are intrinsically dynamic entities, taking part in processes that together span at least eleven orders of magnitude (see Fig. 3) Despite ever-increasing computational power and experimental complexity, there is no single technique that can hope to probe this vast range of timescales. Thus, in this section, we discuss the accessible frequency range of key experimental techniques used to investigate ion dynamics at the interface and highlight the typical processes that they each are tuned to.

3.1.1. Scattering techniques

X-ray and neutron-based scattering techniques are both able to discriminate surface-specific structures and have complementary sensitivities [100,126–129] (Fig. 4(a)-(b)). The interaction between an X-ray photon and an atom scales with the latter's electron density, making it straightforward to detect heavy elements such as rubidium or iodine [33,130]. Conversely, the elements with larger neutron cross-sections tend to be much lighter (e.g. hydrogen, deuterium), and they are thus suited to studies of interfacial liquids such as water [131,132]. The advantage of these techniques lies in their ability to access precisely the region where continuum theories become less robust. Both X-rays and neutrons resolve similar sub-Ångström length scales normal to the interface due to their wavelengths, which are of the same order as crystalline lattice parameters [100,128,131]. This is clearly well-suited to probing interfacial electrolytes, which requires the ability to distinguish ionic binding modes that may be separated by less than the diameter of a single water molecule.

As for most diffraction techniques, the high spatial precision of the interfacial molecular arrangement relies on averaging over large areas of the interface (>mm^2), typically probing in excess of 10^{12} molecules simultaneously. It is therefore necessary for the interface to be homogenous and regular so that single-molecule information is, on average, replicated across the whole region probed.

Temporally, neutron scattering techniques can offer intrinsic dynamic information of the order of picoseconds to nanoseconds [134]. This is complemented by a recent X-ray study that reported

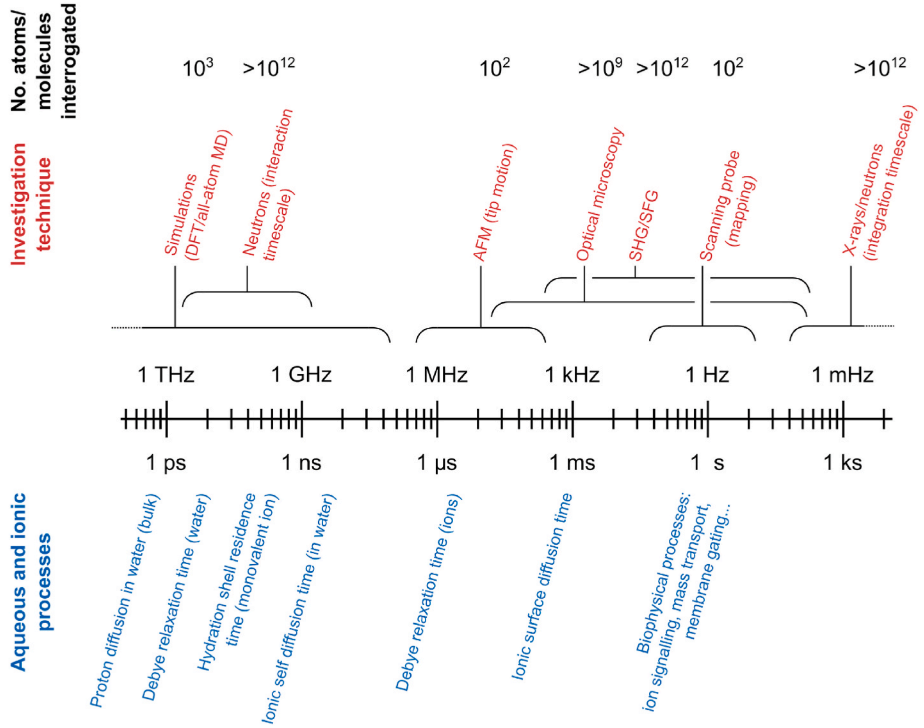

Fig. 3. | The wide-ranging time scales associated with charges at the solid-liquid interface. The approximate timescales of common experimental and computational techniques used to explore aqueous interfaces are illustrated in the upper section (red), along with the typical order of magnitude of the number of molecules interrogated in each case (black). These are compared with the various frequencies related to charge processes in solution (blue) to emphasise the need for both high spatial and temporal resolution when studying such systems. (For interpretation of the references to colour in this figure legend, the reader is referred to the Web version of this article.)

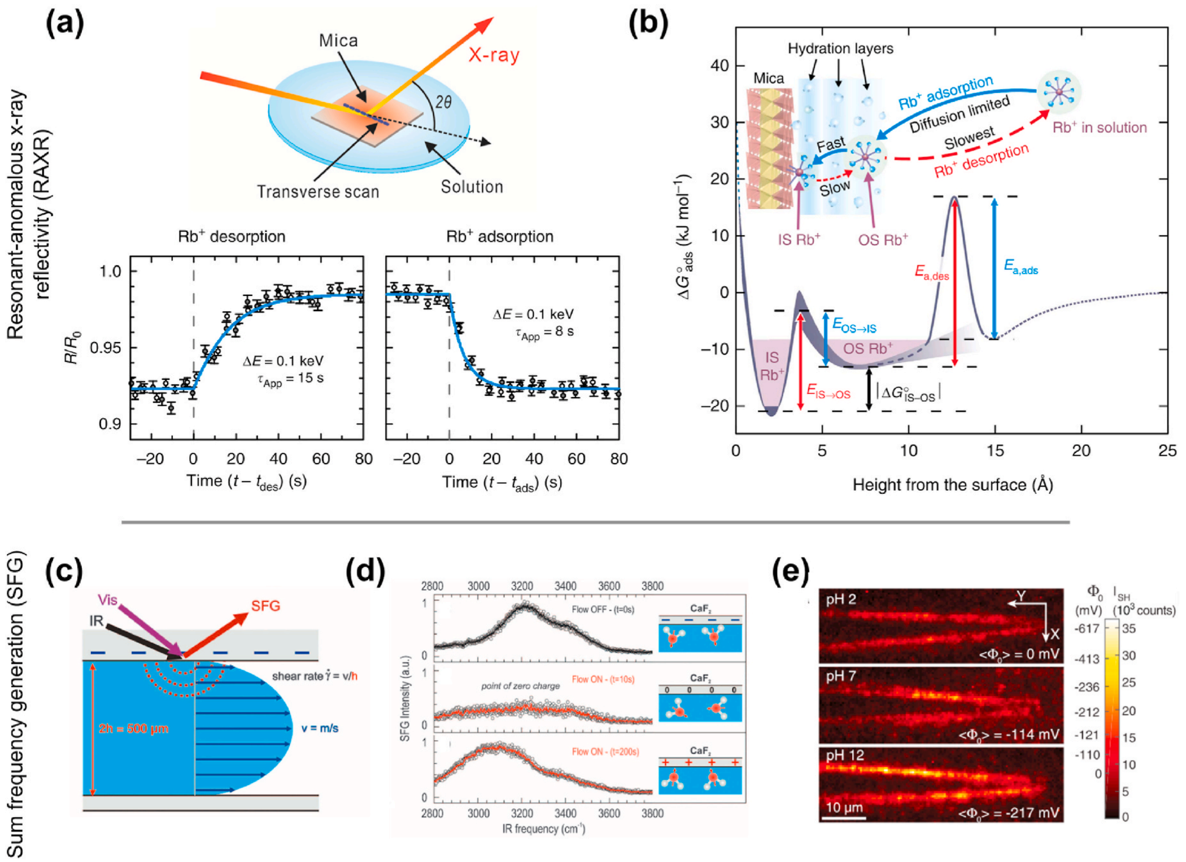

Fig. 4. | Example of nanoscale experimental measurements using photon-based techniques. X-ray and non-linear optical experiments allow for unperturbed, interface-specific studies of the boundary between solids and aqueous solutions, over a variety of time and length-scales. Examples include resonant-anomalous X-ray reflectivity (RAXR, schematic in (a) adapted from Ref. [55]), which have specific sensitivity to heavy elements adsorbed at the Stern layer, allowing for unique measurements of interfacial ionic phenomena. Recent advances in time-resolved RAXR have demonstrated ultra-slow surface ad-/desorption dynamics of Rb^+ ions to mica on the order of seconds ((a), lower), a timescale previously thought to be associated only with ionic equilibrium. This highlighted the decidedly non-trivial energy landscape experienced by ions at the interface, as illustrated in (b) (adapted from Ref. [33]). Non-linear optical techniques such as sum-frequency generation (SFG, schematic in (c)) rely on second-order interactions between two photons and molecules at the interface. These are typically used to probe molecular orientations and vibrations in various aqueous conditions (d, adapted from Ref. [118]), but the development of second-harmonic microscopy has allowed interfacial properties such as surface charge to be mapped in three dimensions, with ~micron resolution and at millisecond timescales (e, adapted from Ref. [133]).

simultaneous sub-molecular (out-of-plane) spatial precision together with second to millisecond temporal resolution [33]. These measurements are however challenging, and spatial averaging remains a key element. The relatively limited interaction of neutrons with matter usually requires long integration times up to hours per Q-value [135]. This typically restricts the dynamic ionic information either to the neutrons' interaction timescale (terahertz to gigahertz), or to the essentially equilibrium experimental timescale (illustrated in Fig. 3). Exciting work on faster neutron beamlines has demonstrated that neutron reflectivity can be used to follow dynamic processes on biological timescales [129,136,137], but there are still challenges with interpreting the results in all four dimensions, including the spatial averaging discussed above. In the specific context of tracking single ions, we note that the incoherent scattering that gives time-domain information is dominated by hydrogens so that dynamic information can only be obtained indirectly by observing dynamic changes in the surrounding waters or performing complementary MD simulations [135].

3.1.2. *Sum frequency generation and non-linear optics*

Non-linear optical techniques allow the study of interfacial fluids at solid surfaces with low-energy photons, avoiding the need for synchrotron sources as in the case of X-ray scattering (Fig. 4(c)–(e)). In the case of sum-frequency generation (SFG), the interface is illuminated with infrared (IR) light, which is energy up-converted by a second incident light source. The reflected signal is proportional to the surface non-linear polarization at the sum of the incident photons' frequencies. This effect is inherently surface-specific and is strongly enhanced at vibrational modes of the interfacial species (~IR frequencies). Hence SFG is well-placed for investigating water molecules' orientation and dynamics at interfaces and around salt ions [66,138–141]. Despite being surface-specific in the out-of-plane (z) direction, typical SFG experiments previously had no lateral resolution, similarly to other spectroscopic techniques. This is no longer the case, with the advent of the second harmonic *microscope*, which allows the mapping of surface chemistry changes on the micron scale [133]. As well as the determination of pK_a values and water structure in confinement, this development has allowed the imaging of hydration and charge on lipid membranes and ion gates with time resolution of ~milliseconds [34,142,143]. This combines truly label-free interrogation of interfacial chemistry and dynamics with a versatile experimental platform and the ability to map large heterogeneous samples, although it currently cannot access the sub-micron to sub-nanometre spatial resolution afforded by scanning probe microscopies.

Because non-linear optical effects are typically second or third order effects, significant photon intensity is generally required to stimulate the system, probe it, or both. This is usually achieved using pulsed lasers [144], with pulses typically in the attosecond to femtosecond domain. By controlling the time delay between the excitation and the probing of a suitable sample, temporal resolution can readily be achieved between femtoseconds up to nanoseconds [145,146]. These approaches are however mainly used to examine vibration modes and electronic redistribution with molecules [147–149], with the excitation wavelength selected to probe the desired physical effects. The most relevant effects to the present review are arguably probed by terahertz spectroscopy of the solvation liquid dynamics [101,150–152], but still orders of magnitude faster than the translation motion of ions along and through interfaces.

3.1.3. Scanning probe techniques

Scanning probe techniques such as scanning tunnelling microscopy [153,154] (STM) or atomic force microscopy (AFM) [155,156] offer unique insight into the structure and dynamics at solid-electrolyte interfaces. The strength of these approaches originates from their atomically sharp probes, which allows them to interrogate only a few (1–100) atoms or molecules at a given interface while still being able to gain contextual information over distances of microns. Measurements can hence be interpreted in terms of molecular or atomistic behaviour at the specific location investigated, typically with sub-nanometre precision [30,35,157,158].

While STM is more famous for its successes in vacuum environment with routine atomic- and even subatomic-level measurements [159,160], the fact that it relies on electrical currents to probe a given sample makes it a tool of choice for molecular electrochemistry. Electrochemical STM studies have, for example, been used to track the atomistic details of electrocatalytic reactions [161,162] the evolution and reconstruction of electrodes in solution under set potentials [163], the structuring of ionic liquids near electrodes [164] or charge transport across metal-electrolyte-metal interfaces [154,165]. Recent technological developments in high-speed STM [166] have improved hardware and software to achieve a temporal resolution in the range of milliseconds to seconds, depending on the system. This temporal resolution is determined by the time it takes for the probe to revisit a set location of the interface while raster-scanning a given region. There is, however, one significant limitation: the reliance on a current between the probe and the solid, which lies at the heart of all STM studies. This means the system is necessarily conductive, and electrochemical processes taking place at the interface must be carefully controlled, limiting the materials, solutions and potentials that can be explored. In practice, electrochemical STM studies tend to rely on atomically flat single crystals as the solid, with the probe remaining as close as possible to the interface.

Instead of currents transferred across the interface, AFM is sensitive to any force experienced by its physical probe, detected *via* the motion of its supporting cantilever (see schematics in Fig. 5). This frees it from many of the constraints of STM; it can operate without restriction on the composition or topography of the solid, and in any liquid transparent enough for its detection laser [156]. Typical interfacial systems range from biological membranes and molecules in a wide range of aqueous solutions [167–170] to minerals and oxides in aqueous and molecular electrolytes [40,50,51,171,172] and conductors and metals in ionic liquids [173–175]. AFM's reliance on a physical, nanoscale tip has direct implications for the accessible length- and timescales. The spatial resolution is controlled by the gradient of the force experienced by the tip and in practice is limited by its sharpness. The specific molecular arrangement of solvent and ions at solid-electrolyte interfaces often induces short-range solvation forces on the measuring tip [171,176,177], hence considerably improving the resolution (as illustrated in Fig. 5(a)). These solvation forces typically decay over a few molecular diameters of the liquid, leading to a situation analogous to STM where the exponentially decaying tunnelling current underpins the outstanding resolution capabilities [178].

Over the last decade, high-resolution AFM has been exploited to map solid-electrolyte interfaces in three dimensions with sub-molecular resolution, probe the solvation structure of solids and adsorbed ions to the extent of discriminating between single adsorbed ions at aqueous interfaces [29,30,35,43–45,117,170,183]. The temporal resolution of AFM is determined by the time it takes for the tip to probe each location

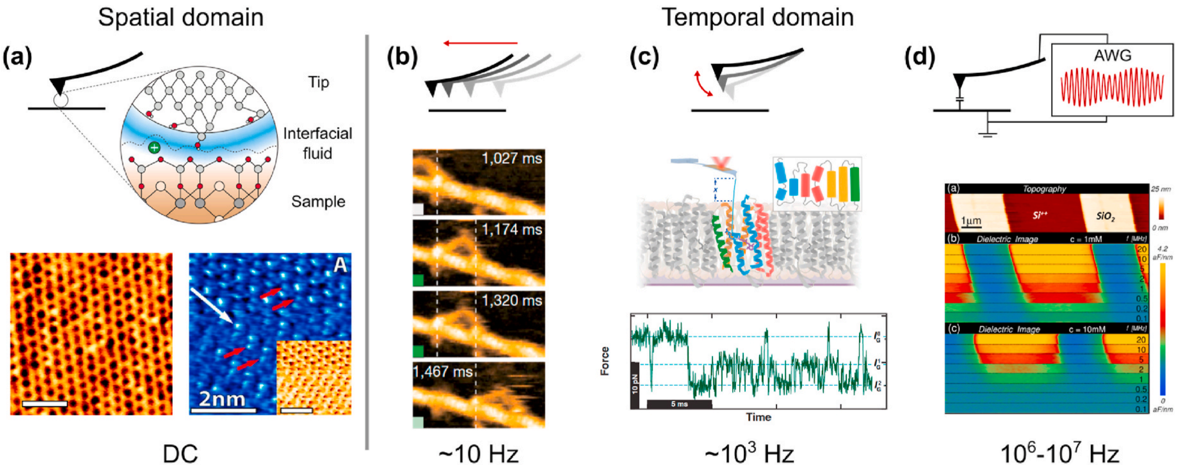

Fig. 5. | The varying scales of spatiotemporal resolution in atomic force microscopy (AFM). (a) Advances in our understanding of the interactions between solids, interfacial fluids and the nano-sharp tips of AFM cantilevers over recent decades has allowed routine atomic (sub-nanometre) spatial resolution to be achieved in liquid. This is exemplified by topographic images of the crystal lattice of muscovite mica by Fukuma *et al.* (lower left, adapted from Ref. [179]) and the discriminating of rubidium cations adsorbed at the surface of calcite in solution by Ricci *et al.* (lower right, red arrows, adapted from Ref. [63]). Regarding temporal resolution, the pioneering work of Ando *et al.* on high-speed (HS) AFM enabled a topographic movie of myosin V walking along actin filaments (b) to be recorded with just ~100 ms between frames (c, adapted from Ref. [180]). Higher temporal resolution can be obtained if spatial information is not needed: by monitoring the forces exerted while stretching bacteriorhodopsin proteins (centre), discrete kinetic transitions between different folding conformations can be observed with sub-millisecond resolution (lower) [181]. (d) Finally, limitations based on the finite response times of AFM probes and control electronics can be somewhat bypassed by instead applying modulated AC electric signals between the probe and the sample with an arbitrary wave generator (AWG). This allows conventional AFM imaging to be conducted while simultaneous dynamical information is obtained through the dielectric response of the sample, with the latter limited only by the electric transfer function of the system. Gramse *et al.* showed that the dielectric gradient (in aF/nm) differences between silicon oxide stripes deposited on doped silicon (Si^{++}) (topography in upper section) could be clearly resolved for modulation frequencies >1 MHz (centre) in 1 mM $KClO_4$ solution (adapted from Ref. [182]). However, as the salt concentration is increased to 10 mM, this actuation frequency rises to ~10 MHz (lower), reflecting the damping produced by the ions' motion within solution. In effect, this allows timescales of order of 10^{-9}-10^{-8} s to be investigated. Scales bar in (a) all represent 2 nm. Scan area in (b) represents 130 × 65 nm^2. (For interpretation of the references to colour in this figure legend, the reader is referred to the Web version of this article.)

of the interface, as for STM. The bandwidth of high-speed AFM [45, 184–189] further depends on the probe's resonance frequency in dynamic operation modes, but it is possible to increase the temporal resolution by restricting the area probed by the tip [43,188,190], or through optimising aspects of the mechanical actuation and hydrodynamics [189]. One of the most notable such developments in high-speed AFM came with the real-time (~100 ms per image) imaging of a myosin molecule "walking" along an actin filament (Fig. 5(b)) [180]. If no spatial information is required (i.e. measuring only the evolution of forces on the tip in time), then resolution can easily reach below the millisecond, vital when attempting to understand e.g. the conformational landscape of proteins [181] (Fig. 5(c)). Further, by directly recording the entire motion of the tip in real time, the available timescale can reach tens of nanoseconds, only limited by the AFM's photodetector and electronics [191,192] (although to date, analysis is non-trivial and must be carried out *post-hoc*). Generally, AFM is presumed to be too slow to capture the motion and dynamics of single ions at interfaces (Fig. 3). However, particular interfaces and solvation structures can dramatically reduce ionic mobility such that individual ions can be tracked over time (more in section 4.2). To explore interfacial dynamics on shorter timescales, it is necessary to bypass the mechanical limitations of the cantilever-probe system altogether. This can be achieved by applying an external electrical or optical stimulus to the sample and detected the stimulus' effect locally with the measuring tip [182,193–197]. The tip itself can be used to apply or enhance the stimulus [31,88,182,195,196]. For example, modulated potentials of arbitrarily high frequencies applied between the tip and the sample (Fig. 5(d)) made it possible to map the dielectric gradient at the silica-electrolyte interface, showing that the dynamics of the $KClO_4$ ions in solution had a major contribution to the measured quantities [182]. Thus, at low molarity (1 mM, Fig. 5(d), centre panel), the dielectric contrast could be clearly observed for modulation frequencies >1 MHz, while at increasing concentrations (10 mM, Fig. 5(d), lower panel), this "actuation" frequency increased to ~10 MHz, reflecting the ions' faster global response time (~100 ns) when they are more abundant. This concentration-dependence is analogous to the Debye timescale of equation (6), describing the ions' ability to respond to an electric field. In practice, it is necessary to take into account multiple aspects of the system to quantify its dynamics including its dielectric response, the ionic diffusion and the system specific geometry [88,92,198,199].

The use of high-frequency electrical fields applied locally at the nanoscale is becoming increasingly popular in scanning probe microscopy [31,88,194,199,200,201], in line with the growing need for local characterisation of electrolyte mobility in energy-related applications. The underlying physics shares many parallels with nanoscale electrical and impendence spectroscopy measurements [92,202–204]. Similarly, the advent of tip-enhanced optical infrared spectroscopies in AFM measurements (nano-IR) shows significant potential to map hydration structures and the molecular organisation of water and ions at solid-liquid interfaces [195–197,205]. This effectively enables optical IR spectroscopy probing of the interfaces with improved sensitivity compared to Fourier Transformed Infrared (FTIR) or SFG, and all while keeping the lateral resolution of AFM.

In parallel, a new family of scanning electrochemical probe microscopies has emerged, taking a different approach from AFM and STM: they directly probe the motion of charges at solid-electrolyte interfaces by flowing a stream of dissolved ions along the interface. These approaches [206,207], which include scanning electrochemical microscopy (SECM), scanning ion conductance microscopy (SICM) and scanning electrochemical cell microscopy (SECCM) among others, rely on an applied electrical potential or pressure which drives ions through a nano-pipette, generating a current. The pipette contains a reference electrode and so can feedback on this ionic current to determine separation from the substrate with no restriction on substrate properties or topography. The spatial resolution is linked to the radius of the pipette [208] and to its ability to concentrate the flux spatially – for example using double-barrelled "theta" pipettes [209] – and usually is in the range 10–100 nm. Here, the main advantage of the technique is the fact that it relies precisely on the motion of ions to map the interface. However, a relatively large number of ions must pass through the pipette to achieve a measurable current (1 pA–10^6-10^7 ions/s) and a sufficient signal-to-noise ratio. This imposes a fundamental limit on the temporal resolution, but with the advantage that ions' response to AC electric fields can be investigated directly and flexibly by applying arbitrary potential waveforms to the electrodes. In general, more molecules and ions are involved in the measurement process than with AFM and temporal resolution tends to be slower although sub-second imaging has been achieved in some cases [208]. This makes SICM measurements suitable for modelling with the PNP formalism, taking into account the specific geometry through finite-element modelling [206,210].

3.2. *Computational techniques*

Computational simulation frameworks effectively function as virtual laboratories, covering the time, length and complexity scales that neither experimental approaches nor analytical methods on the solid-liquid interfaces can access. The level of detail available allows computational techniques to avoid the necessary simplifications present in analytical methods. For instance, simulations are well-suited to solid-liquid interfaces in higher ionic strengths or larger surface charge density situation where e.g. missing ion-ion correlation effects can cause analytical models to fail [104,211,212]. Their robust numerical algorithms allow the interface to be examined in a wide range of conditions with truly atomistic insight into surface structure and dynamics. Additionally, computational techniques retain absolute control over simulated concentrations, chemical species, conditions or any idealisation of the surfaces and fluids which often makes simulations more tractable than experiments. As with all scientific methodologies, simulations have their own idiosyncrasies. Key limitations include the (relatively) short time and length scales accessible, which make it practically impossible to study realistic systems with imperfections to directly compare with experiment. This constrains the results' resolution in parameter space. Further, there can be difficulty in achieving convergent results: this requires the sampling of exhaustive numbers of system states and poses challenges in terms of interpretation of systems. Finally, simulations are only as good as the interaction model they are founded on – i.e. the force fields between each particle. Very many of these force fields were designed and optimised for either crystalline, solid-state systems, or soft matter in contact with bulk electrolytes. Neither of these is strictly applicable to solid-liquid interfaces, the surface chemistry of which is distinct from the bulk phases due to its broken symmetry and the possibility of different protonation states. This introduces uncertainty when performing simulations of these interfaces and care must be taken to ensure conclusions are robust and free from artefacts. Below, we discuss the classical molecular dynamics and coarse-grained simulations, which are the key computational techniques used to explore solid-liquid interfaces. In the context of solid-liquid interfaces, *ab-initio* quantum mechanical simulations tend to be used primarily for establishing the interaction potentials subsequently used in classical simulations and are hence not discussed here.

3.2.1. *Classical molecular dynamics simulations*

Classical molecular dynamics (MD) simulations rely on solving Newtonian equations of motion for every particle in a system, under optimised force fields [213,214] that fold in chemical and physical information on an atomistic level. For over three decades, MD has been used to explore the solid-electrolyte interface, allowing the prediction and explanation of nanoscale processes with a level of precision that is simply not possible with scanning probe microscopies. These simulations offer insights in precisely the regions where the continuum models begin to fail; MD has been used to extend these mean-field models [62, 215,216] and give important insights into both the Stern as well as the diffuse layer, depending on the ionic species involved. Some examples of the information available from MD across a range of systems involving ions is shown in Fig. 6. MD simulations have been extensively used to investigate ions at the interface with minerals (Fig. 6(a)), metals (Fig. 6 (b)) as well as the interfacial dynamics associated with the solvated ions (Fig. 6(c)).

Ideally, MD simulations derive their initial configurations from independent experimental data such as X-ray diffraction techniques [213], but other possibilities, such as simulated annealing [220] are also available. A sampling algorithms is then used to extract the extensive variables that correspond to the ensemble of simulated microscopic systems [221]. Suitable sampling is needed to ensure exploration of all the configurations available to the system: this is not a trivial issue since overcoming energy barriers between different states can be very costly in simulation time [222]. Alternative enhanced sampling approaches such as replica exchange molecular dynamics [223], meta-dynamics [224], parallel tempering [225] and adiabatic dynamics [226] can speed up the free energy barrier crossing. The choice of force field for a given system has to be done carefully since most force fields are calibrated with specific applications in mind. There are only a handful force fields appropriate for interfaces, including the INTERFACE [227] and GoIP [228] force fields, each with their own strengths and shortcomings, that are beyond the scope of this review. The limited availability or accuracy of force fields for specific surfaces have fuelled the idea of obtaining the interatomic forces on-the-fly, in a technique known as ab-initio molecular dynamics (AIMD). AIMD can simulate aqueous interfaces in larger and more complex systems than before [229,230], on similar length and time scales to early classical MD and allowing the study of ion mobility. This may lead to a better description of the interfacial electronic structure and potential polarization effects due to variable charge distributions. In a similar vein, it is worth mentioning polarizable force fields [231–235]. In all cases, proper deployment of classical force fields for solid-liquid interfaces requires treatment of long-range electrostatic interactions, with cut-off rules for non-bonded and short-range electrostatics compatible with those of the force field used for calibration. This information is not traditionally considered as part of the force field but can significantly impact the properties predicted by the simulation.

3.2.2. *Coarse-grained approaches*

Coarse-grained MD has been developed to increase accessible length and time scales in traditional MD simulations. There are various types of coarse-grained models and strategies such as Martini [236], Versatile Object-oriented Toolkit for Coarse-graining Applications (VOTCA) [237], dissipative particle dynamics [238] or self-organized polymer model [239], to name a few. The key approach to coarse-graining entails grouping several atoms or molecules together as a single "bead", with the corresponding interactions calibrated either through all-atom simulations or *via* experimental data. This speeds up calculations simply by requiring fewer particles to describe a system. ,Additionally, the interaction potential might become smoother, bringing further efficiencies [240]. The larger particle masses and the use of constraints also limits the high frequency modes of motion, making the simulations more stable and enabling timesteps up to three orders of magnitude larger than for all-atom MD.

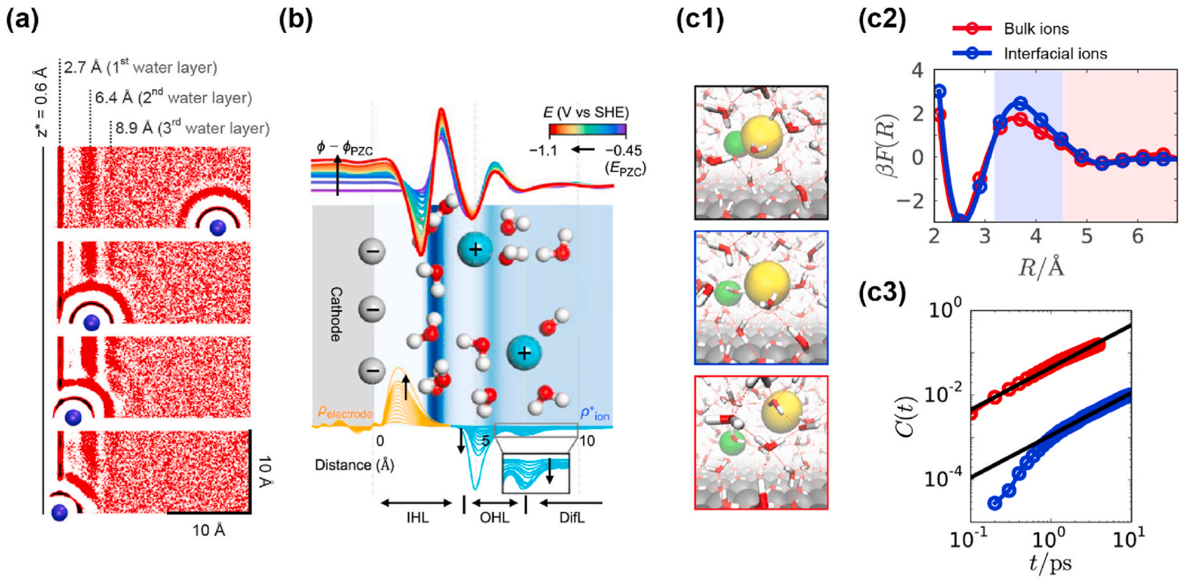

Na$^+$ ions near smectite (montmorillonite)

Na$^+$ ions near an Ag electrode

Na$^+$ & I$^-$ ions at a Pt electrode

Fig. 6. | Molecular dynamics simulations offer a window into the solid-electrolyte interface with atomistic precision | (a) Single sodium cations (purple) have multiple binding sites at the water-smectite interface (corresponding to inner- and outer-Helmholtz layer adsorption; IHL and OHL respectively) that disrupt the native, layered water structure at the crystal's surface oxygens (z*, solid vertical line). Red signifies 1-3 × bulk water density; black signifies >3 × bulk water density. The separation of the water density layers from z* is indicated above the upper panel. (b) Aqueous electrocatalytic systems can also be directly modelled, such as the ionic density dependence of Na$^+$ near an Ag(111) cathode. The layered density of the waters is represented by the blue background gradient, and defines the IHL and OHL (arrows, lower). The system responds dramatically to changes in potential applied to the cathode, with the relative surface potential (rainbow curves, upper), excess charge on the electrode (yellow, lower) and cation density (cyan, lower) all demonstrating clear peaks, especially the alternating layers of ions and waters. (c) Further insight into the dynamics and structure of ions at interfaces can be revealed by free energy calculations as shown here for a system of Na$^+$ and I$^-$ ions and waters at a platinum electrode. In (c1), exemplary snapshots of the bound cation-anion pairs (black border), dissociating ions (blue border) and fully-separated ions (red border) are shown. This process illustrates the free-energy barrier, $\beta F(R)$, between the two states as a function of ion separation, R (c2), with binding occurring at the minima of $R \sim 2.5$ Å. (c3) Interestingly, the minute energetic distinction between these processes in bulk (red) and at the electrode interface (blue) in (c2) results in an enormous change in the ions' dynamics, with the charges dissociating 40 times slower at the interface, as evidenced by their offset correlation functions, $C(t)$. Panel (a) adapted from Ref. [217]; panel (b) from Ref. [218] and panel (c) is from Ref. [219] and copyright of the National Academy of Sciences of the U. S. A. (For interpretation of the references to colour in this figure legend, the reader is referred to the Web version of this article.)

3.3. Exploring ionic motion locally

As clear from sections 3.1 and 3.2, the absolute resolution of a given measurement is not sufficient to determine how localised the obtained information is. Diffraction techniques offer outstanding spatial – and at times also temporal – resolution, but the information is usually averaged over many molecules and ions in-plane and is hence inherently delocalised. Optical and IR spectroscopies excel in gaining temporal information with sufficient resolution to explore molecular vibrational and rotational motions, but also tend to rely on averaging. Recent developments combining spectroscopies with microscopies have drastically reduced the size of the interfacial regions being probed, but the number of molecules or ions interrogated remains large ($>10^6$) with no ability to derive information that can be ascribed to single ions or to specific nanoscale details of an interface such as an atomic defect or topographical feature.

Scanning probe microscopies combine high spatial resolution with truly local measurements by interrogating a small number of molecules or ions (less than ten for the state-of-the-art) at any given location of the interface. Mapping of the interface can be achieved with sub-nanometre resolution, providing key contextual details about the solid's nanoscale topography and chemical composition to support the interpretation of the results in terms of local molecular arrangement or dynamics. However, the ability of scanning probe techniques to operate locally is also a limiting factor for temporal resolution. This is because, as a necessary part of scanning, the nanoscale probe must leave and revisit a given interfacial location to track changes in time, with a delay ranging from tens of milliseconds to minutes. Keeping the probe constantly measuring at a given point can increase temporal resolution but risks influencing the measurement significantly by its physical presence.

Regardless of the technique used, if a high degree of locality is desired, then temporal and spatial resolution are intertwined. This simply reflects the fact that processes occurring over larger length scales in solution require more time, even if they are actively driven (Fig. 3). Consistent with this rule of thumb, smaller molecules or ions generally have greater mobility than their bulkier counterparts for a given environment [241]. This has significant implications for local measurements aiming to track dynamical processes. For example, in order to follow the motion of single ions at solid-electrolyte interfaces, a temporal resolution in the nano-to microsecond is required. Results with existing experimental techniques are only available when system-specific interactions considerably slow down the interfacial dynamics [30,43,44].

Given such stringent physical and technical requirements, it's reasonable to suspect that only *in silico* models can fully describe these systems, with every atomistic detail of the system being tracked at picosecond resolution. At present, there are still limitations imposed by current computing capabilities on the size and duration of simulations, the quality of the sampling, as well as the fact that they rely on approximate interaction potentials; hence experimental validations remain crucial. Ideally, local experimental techniques should complement simulations in as similar a system as possible to fully validate the spatial and temporal picture at the local level. As the emphasis of this review is on *local* tracking, we focus (although not exclusively) on results from scanning probe techniques and simulations.

4. The local equilibrium picture

Most studies examining the organisation and dynamics of ions at solid-liquid interfaces focus on systems at equilibrium. This usually results in capturing a statistical picture of the system, either temporally averaged or representing the most probable molecular configuration. Reviewing our best understanding of these "static" solid-electrolyte interfaces is an obvious starting point, beginning with the organisation of ions perpendicular to the interface before moving to local effects, including in-plane interactions between ions, solvent and the substrate.

4.1. Out-of-plane ionic structure

Substantial progress beyond the double-layer models (section 2.1) began several decades ago, with synchrotron X-rays used to unveil the organisation of water's oxygen atoms at an atomically smooth interface [128,242]. X-ray and neutron diffraction measurements are well-suited to measuring density profiles of solvent molecules and ions at interfaces (see section 3.1.1), with detailed results available over a range of mineral and amorphous interfaces [33,41,48,243,244], electrodes [245,246], as well as soft and biological interfaces [42,126,129,247–250]. In aqueous solutions, these studies identified three distinct water regions: a strongly adsorbed Stern-like region close to the solid, a "hydration" layer adjacent to this, and density oscillations that decay into the bulk fluid. This demonstrated that, even for the simplest of systems, interfacial water could not be approximated as a continuous fluid. Unsurprisingly, the presence of solvated ions was shown to add a further degree of complexity to the interfacial structure [251–253]. For example, divalent strontium ions have two adsorption configurations at the surface of mica in water whereas monovalent rubidium was found to have largely just one [251,252]. These altered hydration states of the adsorbed ions required a strong local reduction of the dielectric constant of water [251], highlighting the variability of parameters usually taken to be global. Such effects are not simply a case of divalent versus monovalent ions but depend on the charge density and specific hydration details of a given ion. X-ray reflectivity studies showed that larger alkali cations such as caesium, rubidium and potassium adsorb directly to mica almost entirely by losing part of their hydration shell (in the so-called *inner-sphere* configuration; equivalent to the inner Helmholtz layer referred to in section 2.1). In contrast, lithium and sodium behave more like divalent ions, with a mix of inner- and outer-sphere adsorption profiles [253,254] (that is, with a finite occupation of the outer Helmholtz layer). These results were borne out by simulations that could further reveal the different in-plane binding sites of Li^+ and Na^+, as well as the intriguing result that smaller cations (with higher charge densities) may have lower effective surface binding affinities due to strongly-bound hydration waters that limit surface interaction [63,255]. For dilute aqueous solutions and negatively charged surfaces, it is generally reasonable to assume that the interface is dominated by cation, water and surface interactions. However, as the ionic strength increases, ion-ion interactions become increasingly important and cannot be excluded [65,256,257]. The onset of this switch from classical to non-classical ionic behaviour was theoretically predicted to occur at a concentration around 1 M for monovalent ions [258], but recent X-ray reflectivity results demonstrated that significant charge overscreening can already occur in a 100 mM aqueous solution of monovalent salts, depending on the system. This was driven by additional anion (Cl^- and I^-) correlations previously thought to be limited to much denser ion solutions and ionic liquids [55]. Such correlations and other non-classical phenomena have been evidenced repeatedly [41,217,255,259] but are still rarely considered when applying EDL models. In fact, charge inversion is even possible in micromolar of a monovalent electrolyte if taking organic ions at hydrophobic surfaces [260]. This result highlights the importance of solvation effects in mediating the interaction of ions with surfaces, and also the fact that the interaction of organic ions with solids can be significantly stronger than that of metal ions [212].

Simulations offer a "direct" way to investigate such non-classical effects at the atomic level, as discussed in section 3.2, and can be used to observe ion-ion lateral and transverse correlations and other properties not accessible through traditional analytical models. Generally, two types of analysis are found in most studies: ionic densities and interfacial properties perpendicular to the surface [261], and the in-plane lateral arrangement of water/ions/dipoles (discussed further in section 4.2). Out-of-plane information is typically averaged over slices parallel to the interface, hence providing information directly comparable to that of diffraction techniques and continuum models. Peaks in the ionic and solvent densities indicates a small number (3–4) of ordered molecular layers that deviate from analytical models, and then rapidly decay to a bulk-like concentration when moving a few nanometres from the interface [30,217,262–270]. This is made clear in Fig. 7(a), where ionic density variations deviate from Gouy-Chapman predictions (black dashed line) and depend sensitively on the species' radius, even for ions of the same charge. The enhanced density of ions in these regions is associated with adsorbed charges that generally perturb the interfacial solvent structure and exhibit higher densities at their most probable hydration states [108,119,217,255,270]. The cooperative ionic arrangement, modified hydration states and the oscillatory solvent behaviour leads to a variation in physico-chemical properties at the interface which are system-specific and demanding predictions from first principles.

Comparison between MD and diffraction-based experimental data often show excellent agreement over the whole interface for out-of-plane average molecular and ionic densities [55,255]. The two families of technique also have the advantage of revealing the "native" arrangement of molecules and ions at the interface and the energy barriers between different configurations, such as bound and unbound states, as in Fig. 6(c2) [219]. This contrasts with techniques based on physical probes, which interrogate the interface precisely by disrupting it. Despite this, diffraction results – probing electron density – tend to agree surprisingly well with those obtained from such "perturbative" techniques as the surface force balance (SFB) and AFM (section 3.1.3), which report on the forces required for the probe to move through the interface. These interactions typically have two key features in both AFM and SFB measurements. The first is a repulsive force that drops off monotonically with probe-interface separation, with exponential decay lengths of ~2–4 Å (see e.g. the results presented for pure water in Fig. 7 (b)). This has become known as the hydration force, due to its comparable length scale to a water molecule's diameter, although not without controversy [36]. This force is remarkably common wherever surfaces are separated by water [36,272] and is distinct from electrostatic interactions [125], being related to the adsorption enthalpy of waters and ions to the surface. The second characteristic component is a much shorter-ranged force that oscillates with separation and reflects the work required to progressively squeeze out molecular layers of water and ions (lower section of Fig. 7(b), corresponding to a solution of 500 mM NaCl). This well-defined structure that forms at the interface is undoubtedly influenced by the confinement of SFB experiments [28,273], but the same oscillations are observed in AFM experiments [32,274,275], even with sharp tips that limit spatial constriction [26,44,276]. This, along with the scattering and simulation results, implies that the inferred molecular organisation is a direct consequence of the topography and chemistry of the interface at equilibrium, rather than an artefact of confinement.

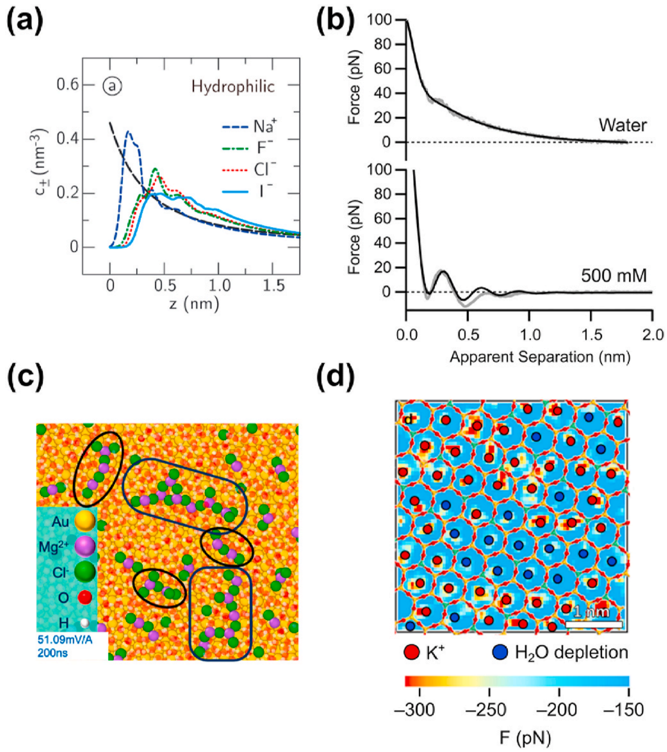

Fig. 7. | Molecular-scale organisation of electrolytes in the vicinity of solid surfaces. Simulations of the interface demonstrate the nanoscale variation in density and structure of charges perpendicular to the interface (a, adapted from Ref. [108]). For small separations ($z < 1.0$ nm) every ion's density clearly deviates from that predicted by Gouy-Chapman theory (black dashes) in a manner that depends both on the sign of the charge and the ionic radius. AFM spectroscopy experiments, (b), replicate this observed layering of ions with remarkable precision, despite the presence of a physical probe (adapted from Ref. [26]). A primarily monotonic hydration repulsion is observed in pure water (upper), but the inclusion of 500 mM NaCl (lower) induces significant oscillatory forces due to interfacial ordering of the ions. (c) The presence of an interface can also lead to ordered in-plane structures: MD studies of $MgCl_2$ at an electrified gold electrode show that subtle field-induced ionic reorganization can create significant ion pairing, in turn driving the formation of Wigner-like crystals without any epitaxial effect from the surface guiding the assembly (adapted from Ref. [65]). Similar non-random ion clusters have been observed experimentally (d), for example in laterally correlated ionic adsorption at muscovite mica, for a KCl concentration of 200 mM (adapted from Ref. [271]). In this case, the ions (red) competed for adsorption sites with interfacial water (blue) and were identified by AFM due to the former's more attractive force induced at $z = 0.3$ nm. (For interpretation of the references to colour in this figure legend, the reader is referred to the Web version of this article.)

Continuum models, which have been the gold standard in the context of solid-electrolyte interfaces for over a century, give us direct predictions about perturbations in counter- and co-ion density (Fig. 1(a)), and so these constitute an obvious reference point. Accordingly, several simulation studies have used MD to measure the ionic distributions near a solid and compared it with continuum models. For example, at an interface between montmorillonite and 100 mM NaCl, the density profiles for Na^+ agreed with a modified Gouy-Chapman theory, but the continuum model overestimated the extent of Cl^- exclusion [215]. The ionic distribution near the interface of a mixed NaCl–$CaCl_2$ solution with smectite, was evaluated using a triple layer model [217] that found charge inversion in the diffusive layer due to contact ion pairs of $CaCl^+$ having a high affinity to the surface. Based on comparison of the Poisson-Boltzmann equation with AIMD results, an implicit solvent model was devised by Bramley *et al.* [277], yielding some encouraging results with agreement between the atomistic description and continuum modelling. There are, however, still important caveats: the exponential form of the Poisson-Boltzmann equation somewhat limits the comparison of analytical and computational models: the boundary conditions of the former are heavily impacted by the counter-ion concentration profile near the surface. This can be calculated through simulations, but in practice it is sensitive to the width of slices used in obtaining average ionic positions. Using very thin slices can eliminate the problem, but acquiring sufficient sampling of ions in each slice requires either prohibitively large simulation boxes or run times. Such agreement between atomistic descriptions and continuum modelling is dependent on using modified or augmented equations that usually require fitted parameters that are not always independently verifiable, hence reducing the predictive power of such models.

Aside from attempting to map the ionic and solvent organisation directly, a key parameter linked indirectly to the interfacial structure is the relative dielectric constant, upon which the majority of continuum models depend sensitively. It is generally agreed that the reduced degrees of freedom close to the solid will dampen ε_r, but there is no generalised model to calculate it for a given interface. This dielectric perturbation has been verified in both simulations [278,279] and experiments [31], affecting the range and magnitude of local electrostatic and surface interactions. For example, a linear relationship between water's relative dielectric constant distribution and its density profile was shown for an aqueous solution of NaCl near the calcite [265]. MD simulations also often distinguish the components of the dielectric constant perpendicular and parallel to the interface [280,281], finding singularities appearing in the perpendicular component.

The out-of-plane ionic structure can also be quantified indirectly through electric characteristics, such as the EDL capacitance, which is a key reference point with continuum models. This capacitance reflects the interface's ability to store electrical energy, and is thus sensitive to the precise arrangement and mobility of ions next to the solid electrodes. The observed capacitance of metal-electrolyte systems in general deviates from the calculated and simulated values due to the specific EDL interactions (see also section 2.3). For example, a recent MD study found it was necessary to tune the "metallicity" of the solid by altering the distribution width of its charges in order to match measured capacitance values [262], affecting the adsorption lifetimes of the ions at the interface. Chemisorption in the Helmholtz layer [269,270,282] can also affect the resulting capacitance of the interface, in particular the presence of a strongly adsorbed water adlayer [283].

From this brief overview of ionic structuring at the electrolyte interface, it is evident that even an equilibrium description of interfacial charges requires careful consideration of the ions' species [30,108,284], valency [63,251], interaction profiles with the solvent and the interface [110,119,285], as well as more thorny concepts such as surface complexation reactions and pH behaviour [49,64,286–288]. This presents a major challenge for continuum models to describe (section 2), especially if considering interfacial phenomena in the Stern or Helmholtz layers. Attempts to comprehensively describe the nature of interfacial ions often rely either on so-called fudge factors and under-determined fitting routines [98], or require so many parameters and prior information that they may as well be a molecular model.

4.2. In-plane organisation and interaction of single ions

While there remains unanswered questions regarding the out of plane organisation of ions at interfaces, the wealth of techniques that can study these systems has led to rapid progress in recent years. A complementary, but much more technologically demanding problem is the *lateral* organisation of electrolytes at interfaces. For example, scattering techniques gain their high out-of-plane spatial resolution by averaging over large areas in-plane, and as such, gaining insight into the lateral organisation of ions and molecules at the interface is challenging. Some studies could quantify lateral correlations within the Stern layer indirectly by fitting adsorption isotherms [30,44,55], but the averaging process usually smears out mesoscale or single-ion phenomena. In contrast, local probe techniques are, by design, able to track nanoscale variations across the interface. Ongoing improvement in dynamic AFM modes has enabled true single-ion resolution at interfaces, with the solid fully immersed into the electrolyte and the measurements conducted at room temperature and even above. Seminal studies demonstrated the technique's ability to image the hydration structure of water and ions at mica and the surface of a gel-phase supported lipid bilayer stably over many seconds [27,170,179,276,289]. Since then, further improvements [35,271,290,291] and the use of several modes of operation have enabled a range of studies tracking the impact of solvated ions on the apparent topography of minerals [40,45,49,52,63,117,120,125,172,183,287,292–294] and the flexible headgroups of lipids in membranes [27,170,276,295,296], all with sub-nanometre resolution. The precise manner in which dissolved ions arranged themselves laterally at interfaces appears to depend far less on "intrinsic" features of the solid such as its surface charge or pK_a than had been previously assumed [297]. For example, single rubidium cations adsorbed at the surface of mica in water exhibit an effective mutual attraction, forming coordinated structures at the interface, despite their similar electrostatic charge [30]. This counterintuitive behaviour is driven by the hydration energy –that is, the free energy due to the ion-water interactions– and is thus remarkably general, not solely limited to charged, crystalline surfaces. This effect can create ion-ion correlations through sharing of some hydration water molecules, thereby releasing more water to the bulk solution and increasing the entropy of the system. Another study has shown a similar behaviour for sodium ions on lipid membranes, thereby also affecting the local mechanical properties of the soft interface [44]. Because these correlation effects are driven by an interplay between the organisation of the water molecules around the ions and the surface of the immersed solid, they depend on the exact type and concentration of ions present and in general can extend over several solvent molecule diameters. Recent development combining high-resolution electrochemical AFM and MD simulations have shown that ions can form correlated ordered structures non-epitaxially or even on amorphous solids, thanks to water-mediated interactions forcing both anions and cations in a limited region of space [65] (simulations highlighted in Fig. 7(c)). 3D mapping of the interface between water and hydrophilic crystals or biological molecules has revealed structured layers of fluid with periodicities similar in scale to water molecules (~0.3 nm) [29,120,176,290,298]. The addition of metal ions to the system induces ion-specific differences [29,293,299], comparable to results from 1D AFM and SFB. This has been used to argue that the measured force is due principally to the tip penetrating strongly adsorbed waters that are structured by the surface [300]. However, many studies are conducted in highly concentrated ionic solutions [120,271,299], and thorough comparison with atomistic models is often required before features can be quantitatively assigned [301]. Overall, AFM studies highlight the importance of a given ion's specific solvation details in determining lateral organisation at the molecular level, but also shows that organised mesoscale ionic structures can modify their local environment and hence interfacial processes [35,43–45,49,297,302].

One key element of these studies is however rarely addressed: the role of the measuring tip [177,303]. For sharp tips (radius of curvature <10 nm), imaging and out of plane AFM measurements have been shown to be largely dominated by the interface, with the tip chemistry having surprisingly little influence [304]. However, atomistic details of the solvation structure at the tip apex can significantly influence the resolution achieved [171,177,300,305,306]. Additionally, since most tips are composed of material that develops a surface charge in solution, it can locally modify the concentration of ions [30], potentially influencing the type and extent of the interfacial ionic structures observed [306]. Interpretation of AFM results is hence often paired with computer simulations of equivalent systems, either without a physical tip [30,120,294,299] or with an explicit model of it [300,301,307,308]. Other approaches include the solvent-tip-approximation (STA) [309], which is a relatively straightforward way to link the forces measured by AFM studies at the interface to the relative density of solvent. This minimalist approach takes advantage of the fact that many high-resolution AFM studies use a tip that is at least partially hydrophilic [177], aiming for the key interaction forces to be dominated by hydration or solvent interactions [300]. The STA thus predicts the measured force from molecular dynamics simulations that model the probe as a single solvent molecule or even extrapolate from equilibrium water density distributions, thus vastly reducing the computational cost [309]. This represents a significant simplification that, while being successful with ultra-sharp, hydrophilic tips, produces results of varying validity [176,300,301]. Direct computation of forces is also possible and relatively accessible, with the use of enhanced sampling techniques [310]. There is usually reasonable agreement with the STA, but better tip representations are sometimes needed [284,301]. More advanced approaches are underway, aiming to circumvent the tip problem using machine learning to map the solid-liquid interface [311,312]. Alternatively, it is possible to explicitly account for the force gradient from 3D AFM data combined with the solid's structure. This is illustrated in Fig. 7(d), where the symmetry of the mica substrate is combined with the strength of the attractive force at $z = 0.3$ nm to classify sites as either having an adsorbed K^+ ion (red) or water depletion (blue).

MD simulations are ideal to visualise the lateral distribution of water and ions on the surface [30,65,297], as illustrated in Fig. 7(c). Findings include the fact that it is the amount of ions in the solvation layers that determine the water structuring at the interface more than the charge density at the surface [313], or that charge inversion is enhanced for multivalent ions [314]. Simulations of water's interface with metallic solids including copper [315–317], gold [262,283], silver [218] and platinum [268,269,283,318,319] showed that water oxygens of the first hydration layer align parallel to the surface, atop the metallic sites. This remains even when electric fields are applied through the fluctuating charge model [267], and also in the present of ions. In most cases a water adlayer on the solid exhibits properties differing from bulk water, and often acts as a barrier to adsorbing ions. The strong adsorption of this adlayer can be due to the polarity of water molecules and epitaxial effects. As a result, small molecules with suitable polarization may be able to form epitaxial adsorption through the first solvation layer, but this is not always the case [65].

A key aspect of the organisation of ions within the Stern layer is the charge-charge correlations that alter the energetics of crystallisation. A recent study on the aggregation of magnesium and chloride ions at the gold-water interface [65] showed that although neither ion tend to adsorb in the first solvation water layer due to unfavourable hydration interactions, stable $MgCl_2$ clusters can form under a transverse electric field. To trigger this assembly, the field induces a small transverse arrangement of the preferred Cl-position, effectively drawing the anions closer to the natural position of the cations. This is sufficient to initiate the formation of stable ionic clusters involving both ions in the second and third solvation layers (Fig. 7(c)), although not the formation of a full ionic lattice as observed experimentally.

Generally, simulations have been extensively used to explore the equilibrium molecular arrangement of solid-electrolyte interfaces, typically revealing the most stable molecular and ionic arrangements and in some cases quantifying their free energy [30,119]. However, it is often not possible to replicate the formation of interfacial structures or assemblies observed experimentally, especially if mesoscale order is present. Comparing orders of magnitude between the size of an experiment over its natural duration with that of a typical simulation returns a ratio $>10^{20}$. Although improved simulation sampling techniques can help bridge this gap, this can be problematic if aiming to capture low probability experimental phenomena such as nucleation processes.

5. Beyond equilibrium: towards the tracking of single ions along interfaces

Up to this point, this review has focused exclusively on equilibrium, time-averaged information. This is partly because most theoretical models, as well as experimental and computational results tend to describe interfaces at equilibrium. Yet, countless processes involving ions at interfaces are inherently time-dependent, usually on a scale faster than accessible with most experimental techniques. Examples range from cell-signalling and bioenergetics in living systems [4–8] to the working of batteries and electrolytic capacitors [320] to nanofluidics [121,259]. There is hence a strong need to increase the temporal resolution of local techniques if to achieve genuine tracking of single ions as they move or organise along interfaces. The relevant time resolution needed for this task typically ranges from nanoseconds [63,65] to seconds [33,43–45], depending on the interactions governing the local ion's dynamics. Hereafter we review some of the recent efforts in that direction and outline possible ways forward for the field.

5.1. Scanning probe microscopies

Despite the development of high-speed AFM [180,321,322], the best temporal resolution achieved with the technique remains in the millisecond realm. While too slow to track freely diffusing ions in bulk, this resolution is still sufficient in many cases to monitor the interactions responsible for the ions adsorbing in the first place. Most mineral and biological surfaces naturally experience strong electrostatic interactions in water due to surface charges or *trans*-interface ionic gradients. As a result, adsorbed ions can remain in a Stern layer long enough to create organised structures, often templated by that of the immersed solid. The first single-ion measurements were achieved on atomically flat mineral surfaces [30,63,172]. Metal ions were shown to adsorb at different locations depending on their charge density and hydration state [43,172]. It was however the larger monovalent ions that appeared more stable in the images, often remaining in place for several consecutive line scans. This unambiguously showed that while electrostatics controls the local ionic concentration and attracts ions to the interface, solvation effects dominate the local organisation and stability, a view consistent with other techniques [33,255,323,324]. The adsorption and desorption kinetics of single rubidium cations could be followed directly [43], showing at the atomic level the competition dynamics with hydronium ions and the resulting differences in the hydration state of the mica surface. The associated timescales, probed with 25 ms temporal resolution, was in the order of 100 ms for the rubidium and 600 ms for the hydronium. These unexpectedly slow dynamics were rationalised by hydration effects whereby the adsorption or desorption of an ions require the simultaneous rearrangement of multiple water molecules. Subsequent temporally resolved diffraction experiments on the same system returned even slower timescales in the order of 10 s, explained by a slow transition between the rubidium's hydration states upon desorption from the interface [33]. Since metal cations are known to form water-mediated networks at the interface with mica [30], the AFM measurements were later extended to track the evolution of entire structures when the interface is under shear flow, showing the flow to impact only fully hydrated ions sitting further from the surface, and the expected slow group dynamics [45]. Similar observations could be made on synthetic lipid membranes [44], revealing an ion-specific interplay between hydration and electrostatic forces that create slowly evolving domains. The residence time of an adsorbed sodium ion in a domain was shown to increase linearly with its number of nearest neighbours, up to tens of seconds for a closed pack arrangement.

These few studies represent the cases where system-specific interactions can dramatically slow down the dynamics of single ions at the interface, rendering direct AFM measurements possible. In the absence of such effects, the interfacial dynamics is likely out of reach with standard setups. One promising way forward entails turning the traditional measurement paradigm around by instead probing the dynamics response of adsorbed ions or charged molecule to a controlled AC electric field applied by a comparatively static AFM tip. The method, analogous to dielectric spectroscopy [325], probes ionic mobilities indirectly, through the changes in the dielectric force experienced by the tip at different location and probing frequencies. The general principles of dielectric force microscopy in solution are presented elsewhere [31,88,193,198,326], but recent developments have shown that it can be used to probe solid-liquid interfaces with nanoscale resolution while simultaneously gathering dielectric information about the adsorbed species at frequencies ranging to the hundreds of MHz (<10 ns) [199]. More developments are needed to derive unambiguous, quantitative information about local ionic mobilities, but the technique is promising. Similarly, nano-IR [195,196,205] which relies on optical rather than electrical stimuli of the interface offers a promising way forward to track changes in the dynamics of charges and molecular arrangement at interfaces with nanoscale precision. Significantly, these advances would finally bridge experimental measurements with MD simulations to run on the same spatial and temporal scale. This would enable direct comparison of the results, including for evolving and out of equilibrium systems.

5.2. Simulations

With a typical time steps of a few femtoseconds, MD simulations can easily track the high-frequency motion of single ions at and along interfaces. Arguably, the main challenge is rather at the opposite end of the spatial and temporal scales: modelling larger systems and for a longer time evolution. At present, MD simulations are still predominantly performed with classical force fields, which permit the investigation of phenomena at length and timescales that generate reasonable sampling of the EDL and transport of ions. The residence time of single ions or water on the surface can be obtained through a statistical approach from equilibrium MD with the use of the time correlation function [262]. Calculation of Mean First Passage Time (MFPT) [119] is another approach which has been deployed in obtaining the desorption time of various ions from a solid surface through MD simulations covering a wide range of desorption times from fs to several seconds.

For interfacial systems consisting of waters and ions, most MD results quantify residence or rearrangement times in order of tens of ps to hundreds of ns [327]. At metal-water interfaces, particularly relevant for technological applications in the field of energy, the water dynamics in the first adlayer covers a range spanning from sub-picoseconds to several nanoseconds. This is highly surface dependent with the persistence time, defined as the waiting time for reorganization events, varying by a factor of 20 between the 100 and 111 facets of platinum [318]. The presence of a surface also dramatically affects charge-charge interactions within the Stern layer, with time-correlation functions demonstrating a reduction by a factor of 40 at the interface, compared with in the bulk [219], as shown in Fig. 6(c3). The difficulty in producing robust, generalisable models is illustrated here by the non-linear nature of the processes: a marked damping of dynamics is driven by a comparatively miniscule difference in the energy barrier between ion binding and decoupling (Fig. 6(c2))

Many non-equilibrium MD studies of water and ions near solid surfaces tend to rely on correlation functions [219], although some studies have investigated the time evolution of the EDL directly, for example the time-dependent Brownian dynamics of various aqueous solutions through a slit, or the hysteresis effect under alternative current due to the formation of ionic pairs in $CaSO_4$ and $CaCl_2$ solutions [122]. However, the derivation of specific relevant statistical mechanics approaches is a central part of non-equilibrium MD approaches, such as the use of different classes of Green-Kubo formula [328,329] to study the non-equilibrium response of interfacial systems under evolving external constraints. These approaches allow the extraction of macroscopic transport variables, but they have yet to be implemented for EDLs.

6. Conclusions and outlook

Our understanding of solvated ions at interfaces has a rich history, dating back to Helmholtz's 19th century work in the context of electrophysiology [69], and continuing to develop through more elaborate modelling and experiment up to the present day. There is much reason to suspect that the field will remain just as salient and lively in the coming decades, even reaching into the 22nd century. Throughout this review, we have sought to emphasise the relevance interfacial ions have to diverse systems, including signalling and energetics in biology; the development of green energy storage systems; and new technology for water de-salination and filtering that will be vital with an uncertain and rapidly changing climate.

The broad relevance of solvated charges has attracted researchers from across the scientific disciplines and generated diverse framings and treatments of the interface. We have discussed the foundational continuum modelling that is routinely used as a point of reference to this day. Such modelling combines well-understood concepts in statistical thermodynamics and electrostatics to arrive at the Poisson-Boltzmann formalism describing ionic distributions near a charged solid. The framework can be extended to capture the time-dependence of processes such as catalysis and electrochemistry, to arrive at the Poisson-Nernst-Planck model. These models endure because of their robustness and versatility but rely on a few key assumptions that break down rather quickly at the interface. In particular, the assumptions that ions have no spatial extent and that the aqueous solvent is homogeneous, with constant dielectric permittivity become increasingly invalid in close proximity to the solid and for moderate ionic strengths. In these conditions, which are commonplace in real-world systems, steric and hydration interactions increasingly dominate the ions' behaviour, and so local, microscopic studies are critical if we are to build a holistic understanding of these interfaces, especially the Stern layer.

We discuss our current best-picture of "equilibrium" ionic structure through examples from experimental and computational techniques that can directly access the interfacial region with the necessary sub-nanometre precision. These techniques have come of age over the past few decades – relatively recently given the long history of research into the EDL. Remarkably, many aspects of the Stern and Helmholtz layer concepts remain broadly correct, despite their one-dimensional, semi-continuum nature. Thus, charged surfaces immersed in electrolyte form at least one highly ordered layer of counterions that were easily distinguished from their bulk concentrations and Poisson-Boltzmann density predictions. However, it has become clear that these ionic layers are *not*, as might reasonably be assumed, purely a result of electrostatic forces, but often dominated by solvation interactions. This leads to a wealth of non-classical ionic phenomena, such as charge over-screening, contact-ion pairs and element-specific ion adsorption and competition.

There have also been important advances in our understanding of in-plane organisation at the interface, including the competition between waters and counterions for adsorption sites and the resulting ion networks that emerge at the meso-scale. The stability of these networks leads naturally to the question of interfacial dynamics: what is the mechanism by which we observe stable structures on the millisecond-second timescale for charges which typically move in bulk with diffusion coefficients of $\sim 10^{-9}$ m^2s^{-1}? A reasonable initial guess is that the structures represent the average densities of a fluctuating ensemble of ions, but the increasing temporal and spatial resolution of AFM indicate this view to be incorrect. The technique's ability to distinguish single adsorbed ions over repeated scan lines has allowed their adsorption kinetics to be followed in real time, demonstrating the power of a hydrophilic interface and competition with waters to reduce their dynamic behaviour. Complementary and independent RAXR results revealed the convoluted energy landscape experienced by interfacial Rb^+ ions that could indeed lead to timescales of seconds to adsorb or desorb.

Due to the technically challenging nature of these single-ion measurements, the use of model, atomically flat solids is a common strategy to simplify the results' interpretation. Recent results have showcased the formation of ordered ionic lattices even at amorphous materials or with ions adsorbed in outer shell configuration with the solvent playing a key role in the ordering. One thing is clear: at present, we are piecing together a microscopic picture of the interface, where element-specific ion-water interactions, relative hydrophilicity of chemical groups, local surface defects, cooperative ionic effects and many more phenomena must be taken into account for a complete description. Given all this, and the plethora of observed non-classical effects, including overscreening, contact ion pairs and in-plane cation networks, is it any surprise that a comprehensive yet general model of the solid-electrolyte interface remains elusive?

The road forward requires technological development to extend the timescales accessible by different surface-specific techniques. This is because there is often little overlap between, e.g. the vibrational frequencies explored by non-linear optical methods and the scanning speeds in atomic force microscopy, as depicted in Fig. 3. As such, we have historically built up a rather siloed picture of ionic motion, where in some contexts, it is appropriate to treat the Stern layer as a frozen sheet of close-packed ions, and in others to consider it as a dynamic, heterogeneous 2D fluid: this will only be resolved by ongoing expansion of the timescales accessible to key experimental techniques. Rather than incremental progress, this will require innovative methodologies and analyses that can overcome the implicit contradictions in our current understanding of ions at solid-liquid interfaces. This could include the application of high-frequency fields during AFM measurements, which augments the technique's single-ion spatial resolution with effective nanosecond temporal resolution of electrical processes. From a computational perspective, access to longer timescales is all but guaranteed, as more powerful processors and efficient algorithms are developed. As well as this however, it is also likely that more complex force fields will need to be developed, perhaps using a multi-scale approach that incorporates the fundamental chemical nature of interfacial species, as with AIMD, but also allows their collective dynamics to be tracked over much longer timescales, as is currently done with coarse-grained approaches. Finally, there is a need for the development of non-equilibrium statistical mechanics approaches specifically tailored to the time-dependent evolution of ions in EDLs.

To summarise the current outlook on the local tracking of solvated ions at interfaces, we believe it is best to mis-quote Feynman [330] and declare that there is plenty more room *in the middle*. That is to say: at one end of the scale, our understanding of the fundamental chemistry, electronic behaviour and vibrational molecular modes at interfaces is relatively mature, as is our fantastically successful continuum picture at the other end. But there remains an abundance of phenomena lying in wait for us at the mesoscale, where the delicate balance between single ion interactions and longer-ranged coordinations persist that are relevant for key biological and energetic processes.

CRediT authorship contribution statement

William Trewby: Writing – review & editing, Writing – original draft, Conceptualization. **Mahdi Tavakol:** Writing – review & editing, Writing – original draft. **Ygor Morais Jaques:** Writing – review & editing, Writing – original draft. **Kislon Voïtchovsky:** Writing – review & editing, Writing – original draft, Supervision, Project administration, Funding acquisition, Conceptualization.

Declaration of competing interest

The authors declare that they have no known competing financial interests or personal relationships that could have appeared to influence the work reported in this paper.

Data availability

This is review. The data is referenced to the initial sources.

Acknowledgements

WT, MT and KV gratefully acknowledge funding from the UK Engineering and Physical Sciences Research Council (grant EP/S028234/1).

References

[1] J.W. Morse, R.S. Arvidson, The dissolution kinetics of major sedimentary carbonate minerals, Earth Sci. Rev. 58 (2002) 51–84.
[2] G. Gonella, et al., Water at charged interfaces, Nat. Rev. Chem 5 (2021) 466–485.
[3] A. Springer, V. Hagen, D. a Cherepanov, Y.N. Antonenko, P. Pohl, Protons migrate along interfacial water without significant contributions from jumps between ionizable groups on the membrane surface, Proc. Natl. Acad. Sci. U.S.A. 108 (2011) 14461–14466.
[4] M. Moustakas, The role of metal ions in biology, Biochemistry and medicine, Materials 14 (2021) 549.
[5] R. Plonsey, Bioelectric phenomena, in: Wiley Encyclopedia of Electrical and Electronics Engineering, John Wiley & Sons, Ltd, 1999, https://doi.org/10.1002/047134608X.W1403.
[6] B. Eisenberg, Interacting ions in biophysics: real is not ideal, Biophys. J. 104 (2013) 1849–1866.
[7] J.J. Shin, C.J. Loewen, Putting the pH into phosphatidic acid signaling, BMC Biol. 9 (2011) 85.
[8] B. Coste, et al., Piezo1 and Piezo2 are essential components of distinct mechanically activated cation channels, Science 330 (2010) 55–60.
[9] W. Kunz, Specific ion effects in colloidal and biological systems, Curr. Opin. Colloid Interface Sci. 15 (2010) 34–39.
[10] Colloid Science: Principles, Methods and Applications, Wiley, Chichester, West Sussex, 2010.
[11] M. von Smoluchowski, Zur kinetischen Theorie der Brownschen Molekularbewegung und der Suspensionen, Ann. Phys. 326 (1906) 756–780.
[12] E. Matijević, S.S. Dukhin, B.V. Derjaguin, A. Mistetsky, M. Zimmerman, Surface and Colloid Science, Wiley-Interscience, New York, 1974.
[13] M.A. Shannon, et al., Science and technology for water purification in the coming decades, Nature 452 (2008) 301–310.
[14] D. Deng, et al., Water purification by shock electrodialysis: deionization, filtration, separation, and disinfection, Desalination 357 (2015) 77–83.
[15] H. Shi, J.A. Lercher, X.-Y. Yu, Sailing into uncharted waters: recent advances in the in situ monitoring of catalytic processes in aqueous environments, Catal. Sci. Technol. 5 (2015) 3035–3060.
[16] K. Xu, Electrolytes, Interfaces and Interphases, The Royal Society of Chemistry, 2023, https://doi.org/10.1039/9781837671311.
[17] C. Prehal, et al., Quantification of ion confinement and desolvation in nanoporous carbon supercapacitors with modelling and in situ X-ray scattering, Nat. Energy 2 (2017) 1–8.
[18] Z. Zhang, et al., Ultrathin and ion-selective janus membranes for high-performance osmotic energy conversion, J. Am. Chem. Soc. 139 (2017) 8905–8914.
[19] P. Simon, Y. Gogotsi, Materials for electrochemical capacitors, Nat. Mater. 7 (2008) 845–854.
[20] G. Li, et al., Enhanced reversible sodium-ion intercalation by synergistic coupling of few-layered MoS $_2$ and S-doped graphene, Adv. Funct. Mater. 27 (2017): 1702562.
[21] D.B. Spry, A. Goun, K. Glusac, D.E. Moilanen, M.D. Fayer, Proton transport and the water environment in nafion fuel cell membranes and AOT reverse micelles, J. Am. Chem. Soc. 129 (2007) 8122–8130.
[22] K. Schmidt-Rohr, Q. Chen, Parallel cylindrical water nanochannels in Nafion fuel-cell membranes, Nat. Mater. 7 (2008) 75–83.
[23] C. Merlet, et al., Highly confined ions store charge more efficiently in supercapacitors, Nat. Commun. 4 (2013) 2701.
[24] L. Cheng, P. Fenter, K.L. Nagy, M.L. Schlegel, N.C. Sturchio, Molecular-scale density oscillations in water adjacent to a mica surface, Phys. Rev. Lett. 87 (2001): 156103.
[25] D.J. Bonthuis, S. Gekle, R.R. Netz, Dielectric profile of interfacial water and its effect on double-layer capacitance, Phys. Rev. Lett. 107 (2011) 1–5.
[26] J.I. Kilpatrick, S.-H. Loh, S.P. Jarvis, Directly probing the effects of ions on hydration forces at interfaces, J. Am. Chem. Soc. 135 (2013) 2628–2634.
[27] M.J. Higgins, et al., Structured water layers adjacent to biological membranes, Biophys. J. 91 (2006) 2532–2542.
[28] J.N. Israelachvili, R.M. Pashley, Molecular layering of water at surfaces and origin of repulsive hydration forces, Nature 306 (1983) 249–250.
[29] D. Martin-Jimenez, E. Chacon, P. Tarazona, R. Garcia, Atomically resolved three-dimensional structures of electrolyte aqueous solutions near a solid surface, Nat. Commun. 7 (2016): 12164.
[30] M. Ricci, P. Spijker, K. Voïtchovsky, Water-induced correlation between single ions imaged at the solid-liquid interface, Nat. Commun. 5 (2014) 4400.
[31] L. Fumagalli, et al., Anomalously low dielectric constant of confined water, Science 360 (2018) 1339–1342.
[32] S.H. Khan, E.L. Kramkowski, P.M. Hoffmann, NaCl-dependent ordering and dynamic mechanical response in nanoconfined water, Langmuir 32 (2016) 10802–10807.
[33] S.S. Lee, P. Fenter, K.L. Nagy, N.C. Sturchio, Real-time observation of cation exchange kinetics and dynamics at the muscovite-water interface, Nat. Commun. 8 (2017): 15826.
[34] O.B. Tarun, M. Yu Eremchev, A. Radenovic, S. Roke, Spatiotemporal imaging of water in operating voltage-gated ion channels reveals the slow motion of interfacial ions, Nano Lett. 19 (2019) 7608–7613.
[35] T. Fukuma, R. Garcia, Atomic- and molecular-resolution mapping of solid–liquid interfaces by 3D atomic force microscopy, ACS Nano 12 (2018) 11785–11797.
[36] V.A. Parsegian, T. Zemb, Hydration forces: observations, explanations, expectations, questions, Curr. Opin. Colloid Interface Sci. 16 (2011) 618–624.
[37] J.N. Israelachvili, Intermolecular and Surface Forces, Elsevier, 2011, https://doi.org/10.1016/C2009-0-21560-1.
[38] P.M. Dove, C.M. Craven, Surface charge density on silica in alkali and alkaline earth chloride electrolyte solutions, Geochem. Cosmochim. Acta 69 (2005) 4963–4970.
[39] C.-J. Yu, et al., Order in molecular liquids near solid–liquid interfaces, Appl. Surf. Sci. 182 (2001) 231–235.
[40] I. Siretanu, et al., Direct observation of ionic structure at solid-liquid interfaces: a deep look into the Stern Layer, Sci. Rep. 4 (2014) 4956.
[41] S.S. Lee, C. Park, N.C. Sturchio, P. Fenter, Nonclassical behavior in competitive ion adsorption at a charged solid–water interface, J. Phys. Chem. Lett. 11 (2020) 4029–4035.
[42] M. Miller, M. Chu, B. Lin, M. Meron, P. Dutta, Observation of ordered structures in counterion layers near wet charged surfaces: a potential mechanism for charge inversion, Langmuir 32 (2016) 73–77.

[43] M. Ricci, W. Trewby, C. Cafolla, K. Voïtchovsky, Direct observation of the dynamics of single metal ions at the interface with solids in aqueous solutions, Sci. Rep. 7 (2017): 43234.

[44] W. Trewby, J. Faraudo, K. Voïtchovsky, Long-lived ionic nano-domains can modulate the stiffness of soft interfaces, Nanoscale 11 (2019) 4376–4384.

[45] C. Cafolla, K. Voïtchovsky, Real-time tracking of ionic nano-domains under shear flow, Sci. Rep. 11 (2021): 19540.

[46] C. Zhao, W. Zheng, A review for aqueous electrochemical supercapacitors, Front. Energy Res. 3 (2015).

[47] L. Collins, et al., Probing charge screening dynamics and electrochemical processes at the solid–liquid interface with electrochemical force microscopy, Nat. Commun. 5 (2014) 3871.

[48] J.E. Stubbs, et al., Epitaxial growth of gibbsite sheets on the basal surface of muscovite mica, J. Phys. Chem. C 123 (2019) 27615–27627.

[49] B.A. Legg, et al., Visualization of aluminum ions at the mica water interface links hydrolysis state-to-surface potential and particle adhesion, J. Am. Chem. Soc. 142 (2020) 6093–6102.

[50] S. Hofmann, K. Voïtchovsky, P. Spijker, M. Schmidt, T. Stumpf, Visualising the molecular alteration of the calcite (104) – water interface by sodium nitrate, Sci. Rep. 6 (2016) 1–11.

[51] M. Ricci, et al., Growth and dissolution of calcite in the presence of adsorbed stearic acid, Langmuir 31 (2015) 7563–7571.

[52] K. Miyata, et al., Variations in atomic-scale step edge structures and dynamics of dissolving calcite in water revealed by high-speed frequency modulation atomic force microscopy, J. Phys. Chem. C 123 (2019) 19786–19793.

[53] K. Voïtchovsky, D. Giofrè, J. José Segura, F. Stellacci, M. Ceriotti, Thermally-nucleated self-assembly of water and alcohol into stable structures at hydrophobic interfaces, Nat. Commun. 7 (2016): 13064.

[54] Solid-Liquid Interfaces: Macroscopic Phenomena, Microscopic Understanding, Springer, Berlin ; New York, 2003.

[55] S.S. Lee, A. Koishi, I.C. Bourg, P. Fenter, Ion correlations drive charge overscreening and heterogeneous nucleation at solid–aqueous electrolyte interfaces, Proc. Natl. Acad. Sci. U.S.A. 118 (2021): e2105154118.

[56] R.R. Netz, Electrofriction and dynamic stern layers at planar charged surfaces, Phys. Rev. Lett. 91 (2003): 138101.

[57] L. Bocquet, E. Charlaix, Nanofluidics, from bulk to interfaces, Chem. Soc. Rev. 39 (2010) 1073–1095.

[58] N. Kavokine, R.R. Netz, L. Bocquet, Fluids at the nanoscale: from continuum to subcontinuum transport, Annu. Rev. Fluid Mech. 53 (2021) 377–410.

[59] M.S. Kilic, M.Z. Bazant, A. Ajdari, Steric effects in the dynamics of electrolytes at large applied voltages. I. Double-layer charging, Phys. Rev. E 75 (2007): 021502.

[60] C. Merlet, et al., On the molecular origin of supercapacitance in nanoporous carbon electrodes, Nat. Mater. 11 (2012) 306–310.

[61] Q. Tan, et al., Experimental observation of the ion–ion correlation effects on charge inversion and strong adhesion between mica surfaces in aqueous electrolyte solutions, Langmuir 30 (2014) 10845–10854.

[62] R. Hartkamp, B. Siboulet, J.F. Dufrêche, B. Coasne, Ion-specific adsorption and electroosmosis in charged amorphous porous silica, Phys. Chem. Chem. Phys. 17 (2015) 24683–24695.

[63] M. Ricci, P. Spijker, F. Stellacci, J.-F. Molinari, K. Voïtchovsky, Direct visualization of single ions in the stern layer of calcite, Langmuir 29 (2013) 2207–2216.

[64] C. Zhao, D. Ebeling, I. Siretanu, D. van den Ende, F. Mugele, Extracting local surface charges and charge regulation behavior from atomic force microscopy measurements at heterogeneous solid-electrolyte interfaces, Nanoscale 7 (2015) 16298–16311.

[65] J. Wang, et al., Ions adsorbed at amorphous solid/solution interfaces form wigner crystal-like structures, ACS Nano 18 (2024) 1181–1194.

[66] F. Zaera, Probing liquid/solid interfaces at the molecular level, Chem. Rev. 112 (2012) 2920–2986.

[67] M. Radiom, Ionic liquid–solid interface and applications in lubrication and energy storage, Curr. Opin. Colloid Interface Sci. 39 (2019) 148–161.

[68] R. Hayes, G.G. Warr, R. Atkin, Structure and nanostructure in ionic liquids, Chem. Rev. 115 (2015) 6357–6426.

[69] Hermann Helmholtz, Ueber einige Gesetze der Vertheilung elektrischer Ströme in körperlichen Leitern mit Anwendung auf die thierisch-elektrischen Versuche, Ann. Phys. Chem. 89 (1853) 211–233.

[70] M. Gouy, Sur la constitution de la charge électrique à la surface d'un électrolyte, J. Phys. Theor. Appl. 9 (1910) 457–468.

[71] D.L. Chapman, A contribution to the theory of electrocapillarity, London, Edinburgh Dublin Phil. Mag. J. Sci. 25 (1913) 475–481.

[72] J.C. Berg, An Introduction to Interfaces and Colloids: the Bridge to Nanoscience, World Scientific Publishing Co., 2009.

[73] H.-J. Butt, K. Graf, M. Kappl, Physics and Chemistry of Interfaces, Wiley-VCH, 2003.

[74] Y. Uematsu, Electrification of water interface, J. Phys. Condens. Matter 33 (2021): 423001.

[75] O. Stern, Zur theorie der elektrolytischen doppelschicht. Z. Für elektrochem, Angew. Phys. Chem. 30 (1924) 508–516.

[76] D.C. Grahame, The electrical double layer and the theory of electrocapillarity, Chem. Rev. 41 (1947) 441–501.

[77] S. Casalini, C.A. Bortolotti, F. Leonardi, F. Biscarini, Self-assembled monolayers in organic electronics, Chem. Soc. Rev. 46 (2017) 40–71.

[78] K. Choi, et al., A short review on interface engineering of perovskite solar cells: a self-assembled monolayer and its roles, Sol. RRL 4 (2020): 1900251.

[79] S. Lin, X. Chen, Z.L. Wang, Contact electrification at the liquid–solid interface, Chem. Rev. 122 (2022) 5209–5232.

[80] P. Debye, E. Hückel, Zur Theorie der Elektrolyte. I. Gefrierpunktserniedrigung und verwandte Erscheinungen, Phys. Z. 24 (1923) 185–206.

[81] R.B. Schoch, J. Han, P. Renaud, Transport phenomena in nanofluidics, Rev. Mod. Phys. 80 (2008) 839–883.

[82] A.V. Delgado, F. González-Caballero, R.J. Hunter, L.K. Koopal, J. Lyklema, Measurement and interpretation of electrokinetic phenomena, J. Colloid Interface Sci. 309 (2007) 194–224.

[83] F.H.J. van der Heyden, D. Stein, C. Dekker, Streaming currents in a single nanofluidic channel, Phys. Rev. Lett. 95 (2005): 116104.

[84] M.Z. Bazant, M.S. Kilic, B.D. Storey, A. Ajdari, Towards an understanding of induced-charge electrokinetics at large applied voltages in concentrated solutions, Adv. Colloid Interface Sci. 152 (2009) 48–88.

[85] M.Z. Bazant, K. Thornton, A. Ajdari, Diffuse-charge dynamics in electrochemical systems, Phys. Rev. E 70 (2004): 021506.

[86] L. Højgaard Olesen, M.Z. Bazant, H. Bruus, Strongly nonlinear dynamics of electrolytes in large ac voltages, Phys. Rev. E 82 (2010): 011501.

[87] P.M. Biesheuvel, M.Z. Bazant, Nonlinear dynamics of capacitive charging and desalination by porous electrodes, Phys. Rev. E 81 (2010): 031502.

[88] R. Millan-Solsona, M. Checa, L. Fumagalli, G. Gomila, Mapping the capacitance of self-assembled monolayers at metal/electrolyte interfaces at the nanoscale by in-liquid scanning dielectric microscopy, Nanoscale 12 (2020) 20658–20668.

[89] L. Huetter, A. Kyndiah, G. Gomila, Analytical physical model for organic metal-electrolyte-semiconductor capacitors, Adv. Theory Simul. 6 (2023): 2200698.

[90] Ł. Richter, et al., Ions in an AC electric field: strong long-range repulsion between oppositely charged surfaces, Phys. Rev. Lett. 125 (2020): 056001.

[91] L. Collins, J.I. Kilpatrick, S.V. Kalinin, B.J. Rodriguez, Towards nanoscale electrical measurements in liquid by advanced KPFM techniques: a review, Rep. Prog. Phys. 81 (2018): 086101.

[92] M. Saghafi, S. Chinnathambi, S.G. Lemay, High-frequency phenomena and electrochemical impedance spectroscopy at nanoelectrodes, Curr. Opin. Colloid Interface Sci. 63 (2023): 101654.

[93] M.A. Brown, G.V. Bossa, S. May, Emergence of a stern layer from the incorporation of hydration interactions into the gouy-chapman model of the electrical double layer, Langmuir 31 (2015) 11477–11483.

[94] W. Bu, D. Vaknin, A. Travesset, How accurate is Poisson−Boltzmann theory for monovalent ions near highly charged interfaces? Langmuir 22 (2006) 5673–5681.

[95] S. McLaughlin, The electrostatic properties of membranes, Annu. Rev. Biophys. Biomol. Struct. 18 (1989) 113–136.

[96] J.M. Bloch, W. Yun, Condensation of monovalent and divalent metal ions on a Langmuir monolayer, Phys. Rev. 41 (1990) 844–862.

[97] M. Předota, M.L. Machesky, D.J. Wesolowski, Molecular origins of the zeta potential, Langmuir 32 (2016).

[98] R. Hartkamp, et al., Measuring surface charge: why experimental characterization and molecular modeling should be coupled, Curr. Opin. Colloid Interface Sci. 37 (2018) 101–114.

[99] S. Kumar, et al., Absence of anomalous underscreening in highly concentrated aqueous electrolytes confined between smooth silica surfaces, J. Colloid Interface Sci. 622 (2022) 819–827.

[100] K.D. Collins, G.W. Neilson, J.E. Enderby, Ions in water: characterizing the forces that control chemical processes and biological structure, Biophys. Chem. 128 (2007) 95–104.

[101] G. Schwaab, F. Sebastiani, M. Havenith, Ion hydration and ion pairing as probed by THz spectroscopy, Angew. Chem. Int. Ed. 58 (2019) 3000–3013.

[102] H. Boroudjerdi, et al., Statics and dynamics of strongly charged soft matter, Phys. Rep. 416 (2005) 129–199.

[103] A. Grosberg, T. Nguyen, B. Shklovskii, Colloquium: the physics of charge inversion in chemical and biological systems, Rev. Mod. Phys. 74 (2002) 329–345.

[104] J. Faraudo, A. Travesset, The many origins of charge inversion in electrolyte solutions: effects of discrete interfacial charges, J. Phys. Chem. C 111 (2007) 987–994.

[105] R.R. Netz, H. Orland, Beyond Poisson-Boltzmann: fluctuation effects and correlation functions, Eur. Phys. J. E 1 (2000) 203–214.

[106] C.S. Perez-Martinez, S. Perkin, Surface forces generated by the action of electric fields across liquid films, Soft Matter 15 (2019) 4255–4265.

[107] S.M.H. Hashemi Amrei, S.C. Bukosky, S.P. Rader, W.D. Ristenpart, G.H. Miller, Oscillating electric fields in liquids create a long-range steady field, Phys. Rev. Lett. 121 (2018): 185504.

[108] D.J. Bonthuis, R.R. Netz, Beyond the continuum: how molecular solvent structure affects electrostatics and hydrodynamics at solid–electrolyte interfaces, J. Phys. Chem. B 117 (2013) 11397–11413.

[109] Y. Marcus, Effect of ions on the structure of water: structure making and breaking, Chem. Rev. 109 (2009) 1346–1370.

[110] N. Schwierz, D. Horinek, R.R. Netz, Anionic and cationic hofmeister effects on hydrophobic and hydrophilic surfaces, Langmuir 29 (2013) 2602–2614.

[111] Y. Zhang, P.S. Cremer, Interactions between macromolecules and ions: the Hofmeister series, Curr. Opin. Chem. Biol. 10 (2006) 658–663.

[112] A. Tuladhar, et al., Ions tune interfacial water structure and modulate hydrophobic interactions at silica surfaces, J. Am. Chem. Soc. 142 (2020) 6991–7000.

[113] B. Eisenberg, Ionic interactions are everywhere, Physiology 28 (2013) 28–38.

[114] T. Del Castillo-Santaella, J. Maldonado-Valderrama, J. Faraudo, A. Martín-Molina, Specific ion effects in cholesterol monolayers, Materials 9 (2016) 340.

[115] A. Aroti, E. Leontidis, M. Dubois, T. Zemb, Effects of monovalent anions of the hofmeister series on DPPC lipid bilayers Part I: swelling and in-plane equations of state, Biophys. J. 93 (2007) 1580–1590.

[116] H. Petrache, T. Zemb, L. Belloni, V. Parsegian, Salt screening and specific ion adsorption determine neutral-lipid membrane interactions, Proc. Natl. Acad. Sci. U.S.A. 103 (2006) 7982–7987.

[117] I. Siretanu, D. van den Ende, F. Mugele, Atomic structure and surface defects at mineral-water interfaces probed by in situ atomic force microscopy, Nanoscale 8 (2016) 8220–8227.

[118] D. Lis, E.H.G. Backus, J. Hunger, S.H. Parekh, M. Bonn, Liquid flow along a solid surface reversibly alters interfacial chemistry, Science 344 (2014) 1138–1142.

[119] S. Hocine, et al., How ion condensation occurs at a charged surface: a molecular dynamics investigation of the stern layer for water–silica interfaces, J. Phys. Chem. C 120 (2016) 963–973.

[120] K. Umeda, et al., Atomic-resolution three-dimensional hydration structures on a heterogeneously charged surface, Nat. Commun. 8 (2017) 2111.

[121] L. Bocquet, Nanofluidics coming of age, Nat. Mater. 19 (2020) 254–256.

[122] P. Robin, N. Kavokine, L. Bocquet, Modeling of emergent memory and voltage spiking in ionic transport through angstrom-scale slits, Science 373 (2021) 687–691.

[123] N. Kavokine, M.-L. Bocquet, L. Bocquet, Fluctuation-induced quantum friction in nanoscale water flows, Nature 602 (2022) 84–90.

[124] T.H.N. Minh, B. Rotenberg, S. Marbach, Ionic fluctuations in finite volumes: fractional noise and hyperuniformity, Faraday Discuss 246 (2023) 225–250.

[125] A. Klaassen, F. Liu, F. Mugele, I. Siretanu, Correlation between electrostatic and hydration forces on silica and gibbsite surfaces: an atomic force microscopy study, Langmuir 38 (2022) 914–926.

[126] M.J. Bedzyk, G.M. Bommarito, M. Caffrey, T.L. Penner, Diffuse-double layer at a membrane-aqueous interface measured with X-ray standing waves, Science 248 (1990) 52–56.

[127] E. Schneck, B. Demé, Structural characterization of soft interfaces by standing-wave fluorescence with X-rays and neutrons, Curr. Opin. Colloid Interface Sci. 20 (2015) 244–252.

[128] P. Fenter, N.C. Sturchio, Mineral-water interfacial structures revealed by synchrotron X-ray scattering, Prog. Surf. Sci. 77 (2005) 171–258.

[129] J.H. Lakey, Recent advances in neutron reflectivity studies of biological membranes, Curr. Opin. Colloid Interface Sci. 42 (2019) 33–40.

[130] S.J.T. Brugman, E.R. Townsend, M.M.H. Smets, P. Accordini, E. Vlieg, Concentration-dependent adsorption of CsI at the muscovite–electrolyte interface, Langmuir 34 (2018) 3821–3826.

[131] M.L. Martins, et al., Neutron scattering, a powerful tool to study clay minerals, Appl. Clay Sci. 96 (2014) 22–35.

[132] T. Yamada, H. Seto, Quasi-Elastic neutron scattering studies on hydration water in phospholipid membranes, Front. Chem. 8 (2020) 8.

[133] C. Macias-Romero, I. Nahalka, H.I. Okur, S. Roke, Optical imaging of surface chemistry and dynamics in confinement, Science 357 (2017) 784–788.

[134] P. Porion, et al., Water and ion dynamics in confined media: a multi-scale study of the clay/water interface, Colloids Interf 5 (2021) 34.

[135] L.J. Michot, E. Ferrage, M. Jiménez-Ruiz, M. Boehm, A. Delville, Anisotropic features of water and ion dynamics in synthetic Na- and Ca-smectites with tetrahedral layer charge. A combined quasi-elastic neutron-scattering and molecular dynamics simulations study, J. Phys. Chem. C 116 (2012) 16619–16633.

[136] F.A. Adlmann, et al., Towards neutron scattering experiments with sub-millisecond time resolution, J. Appl. Crystallogr. 48 (2015) 220–226.

[137] A. Koutsioubas, M.-S. Appavou, D. Lairez, Time-resolved neutron reflectivity during supported membrane formation by vesicle fusion, Langmuir 33 (2017) 10598–10605.

[138] S.C. Flores, J. Kherb, N. Konelick, X. Chen, P.S. Cremer, The effects of hofmeister cations at negatively charged hydrophilic surfaces, J. Phys. Chem. C 116 (2012) 5730–5734.

[139] K.C. Jena, P.A. Covert, D.K. Hore, The effect of salt on the water structure at a charged solid surface: differentiating second- and third-order nonlinear contributions, J. Phys. Chem. Lett. 2 (2011) 1056–1061.

[140] M. Bischoff, D. Biriukov, M. Předota, S. Roke, A. Marchioro, Surface potential and interfacial water order at the amorphous TiO_2 nanoparticle/aqueous interface, J. Phys. Chem. C 124 (2020) 10961–10974.

[141] B. Rehl, et al., Water structure in the electrical double layer and the contributions to the total interfacial potential at different surface charge densities, J. Am. Chem. Soc. 144 (2022) 16338–16349.

[142] O.B. Tarun, C. Hannesschläger, P. Pohl, S. Roke, Label-free and charge-sensitive dynamic imaging of lipid membrane hydration on millisecond time scales, Proc. Natl. Acad. Sci. USA 115 (2018) 4081–4086.

[143] O.B. Tarun, H.I. Okur, P. Rangamani, S. Roke, Transient domains of ordered water induced by divalent ions lead to lipid membrane curvature fluctuations, Commun. Chem. 3 (2020) 17.

[144] M. Maiuri, M. Garavelli, G. Cerullo, Ultrafast spectroscopy: state of the art and open challenges, J. Am. Chem. Soc. 142 (2020) 3–15.

[145] S. Mukamel, Principles of Nonlinear Optical Spectroscopy, Oxford Univ. Press, New York, 2009.

[146] A. Bhattacharya, Ultrafast Optics and Spectroscopy in Physical Chemistry, World Scientific, New Jersey, 2018.

[147] M.F. Kropman, H.J. Bakker, Dynamics of water molecules in aqueous solvation shells, Science 291 (2001) 2118–2120.

[148] M. Khalil, N. Demirdöven, A. Tokmakoff, Coherent 2D IR spectroscopy: molecular structure and dynamics in solution, J. Phys. Chem. A 107 (2003) 5258–5279.

[149] I. Jordan, et al., Attosecond spectroscopy of liquid water, Science 369 (2020) 974–979.

[150] M.C. Beard, G.M. Turner, C.A. Schmuttenmaer, Terahertz spectroscopy, J. Phys. Chem. B 106 (2002) 7146–7159.

[151] M. Śmiechowski, J. Sun, H. Forbert, D. Marx, Solvation shell resolved THz spectra of simple aqua ions – distinct distance- and frequency-dependent contributions of solvation shells, Phys. Chem. Chem. Phys. 17 (2015) 8323–8329.

[152] D.A. Schmidt, et al., Rattling in the cage: ions as probes of sub-picosecond water network dynamics, J. Am. Chem. Soc. 131 (2009) 18512–18517.

[153] G. Binnig, H. Rohrer, Scanning tunneling microscopy, Helv. Phys. Acta 55 (1982) 726–735.

[154] K. Itaya, In situ scanning tunneling microscopy in electrolyte solutions, Prog. Surf. Sci. 58 (1998) 121–247.

[155] G. Binnig, C.F. Quate, Ch Gerber, Atomic force microscope, Phys. Rev. Lett. 56 (1986) 930–933.

[156] R. García, Amplitude Modulation Atomic Force Microscopy, Wiley-VCH Verlag GmbH & Co. KGaA, Weinheim, Germany, 2010, https://doi.org/10.1002/9783527632183.

[157] G.R. Heath, et al., Localization atomic force microscopy, Nature 594 (2021) 385–390.

[158] A. Pyne, R. Thompson, C. Leung, D. Roy, B.W. Hoogenboom, Single-molecule reconstruction of oligonucleotide secondary structure by atomic force microscopy, Small 10 (2014) 3257–3261.

[159] J. Repp, G. Meyer, S.M. Stojković, A. Gourdon, C. Joachim, Molecules on insulating films: scanning-tunneling microscopy imaging of individual molecular orbitals, Phys. Rev. Lett. 94 (2005): 026803.

[160] F. Mohn, L. Gross, N. Moll, G. Meyer, Imaging the charge distribution within a single molecule, Nat. Nanotechnol. 7 (2012) 227–231.

[161] Y. Wang, S.A. Skaanvik, X. Xiong, S. Wang, M. Dong, Scanning probe microscopy for electrocatalysis, Matter 4 (2021) 3483–3514.

[162] Y. Liang, et al., Electrochemical scanning probe microscopies in electrocatalysis, Small Methods 3 (2019): 1800387.

[163] Y.-G. Kim, J.Y. Kim, D. Vairavapandian, J.L. Stickney, Platinum nanofilm formation by EC-ALE via redox replacement of UPD copper: studies using in-situ scanning tunneling microscopy, J. Phys. Chem. B 110 (2006) 17998–18006.

[164] T. Pajkossy, C. Müller, T. Jacob, The metal–ionic liquid interface as characterized by impedance spectroscopy and in situ scanning tunneling microscopy, Phys. Chem. Chem. Phys. 20 (2018) 21241–21250.

[165] H. Feng, X. Xu, Y. Du, S.X. Dou, Application of scanning tunneling microscopy in electrocatalysis and electrochemistry, Electrochem. Energy Rev. 4 (2021) 249–268.

[166] L. Gura, et al., Resolving atomic diffusion in Ru(0001)−O(2×2) with spiral high-speed scanning tunneling microscopy, Phys. Rev. B 105 (2022): 035411.

[167] Y.-C. Lin, et al., Force-induced conformational changes in PIEZO1, Nature 573 (2019) 230–234.

[168] A.P. Perrino, R. Garcia, How soft is a single protein? The stress-strain curve of antibody pentamers with 5 pN and 50 pm resolutions, Nanoscale 8 (2016) 9151–9158.

[169] S.A. Contera, K. Voïtchovsky, J.F. Ryan, Controlled ionic condensation at the surface of a native extremophile membrane, Nanoscale 2 (2010) 222–229.

[170] T. Fukuma, M. Higgins, S. Jarvis, Direct imaging of lipid-ion network formation under physiological conditions by frequency modulation atomic force microscopy, Phys. Rev. Lett. 98 (2007): 106101.

[171] K. Voïtchovsky, J.J. Kuna, S.A. Contera, E. Tosatti, F. Stellacci, Direct mapping of the solid-liquid adhesion energy with subnanometre resolution, Nat. Nanotechnol. 5 (2010) 401–405.

[172] S.H. Loh, S.P. Jarvis, Visualization of ion distribution at the mica-electrolyte interface, Langmuir 26 (2010) 9176–9178.

[173] J.A Page, et al., 3-Dimensional atomic scale structure of the ionic liquid–graphite interface elucidated by AM-AFM and quantum chemical simulations, Nanoscale 6 (2014) 8100–8106.

[174] S. Mcdonald, A. Elbourne, G.G. Warr, R. Atkin, Metal ion adsorption at the ionic liquid–mica interface, Nanoscale 8 (2015) 906–914.

[175] R. Atkin, et al., AFM and STM studies on the surface interaction of [BMP]TFSA and [EMIm]TFSA ionic liquids with Au(111), J. Phys. Chem. C 113 (2009) 13266–13272.

[176] K. Miyazawa, et al., A relationship between three-dimensional surface hydration structures and force distribution measured by atomic force microscopy, Nanoscale 8 (2016) 7334–7342.

[177] S.M.R. Akrami, H. Nakayachi, T. Watanabe-Nakayama, H. Asakawa, T. Fukuma, Significant improvements in stability and reproducibility of atomic-scale atomic force microscopy in liquid, Nanotechnology 25 (2014): 455701.

[178] G. Binnig, H. Rohrer, Ch Gerber, E. Weibel, Surface studies by scanning tunneling microscopy, Phys. Rev. Lett. 49 (1982) 57–61.

[179] T. Fukuma, K. Kobayashi, K. Matsushige, H. Yamada, True atomic resolution in liquid by frequency-modulation atomic force microscopy, Appl. Phys. Lett. 87 (2005): 034101.

[180] N. Kodera, D. Yamamoto, R. Ishikawa, T. Ando, Video imaging of walking myosin V by high-speed atomic force microscopy, Nature 468 (2010) 72–76.

[181] H. Yu, D.R. Jacobson, H. Luo, T.T. Perkins, Quantifying the native energetics stabilizing bacteriorhodopsin by single-molecule force spectroscopy, Phys. Rev. Lett. 125 (2020): 068102.

[182] G. Gramse, M.A. Edwards, L. Fumagalli, G. Gomila, Dynamic electrostatic force microscopy in liquid media, Appl. Phys. Lett. 101 (2012): 213108.

[183] C. Cafolla, K. Voïtchovsky, Lubricating properties of single metal ions at interfaces, Nanoscale 10 (2018) 11831–11840.

[184] A. Colom, I. Casuso, F. Rico, S. Scheuring, A hybrid high-speed atomic force-optical microscope for visualizing single membrane proteins on eukaryotic cells, Nat. Commun. 4 (2013) 2155.

[185] I. Munguira, et al., Glasslike membrane protein diffusion in a crowded membrane, ACS Nano 10 (2016) 2584–2590.

[186] T. Uchihashi, R. Iino, T. Ando, H. Noji, High-speed atomic force microscopy reveals rotary catalysis of rotorless F1-ATPase, Science 333 (2011) 755–758.

[187] K. Miyata, et al., High-speed atomic force microscopy of the structure and dynamics of calcite nanoscale etch pits, J. Phys. Chem. Lett. 12 (2021) 8039–8045.

[188] G.R. Heath, S. Scheuring, High-speed AFM height spectroscopy reveals µs-dynamics of unlabeled biomolecules, Nat. Commun. 9 (2018) 4983.

[189] T. Ando, High-speed atomic force microscopy coming of age, Nanotechnology 23 (2012): 062001.

[190] M.B. Viani, et al., Probing protein-protein interactions in real time, Nat. Struct. Biol. 7 (2000) 644–647.

[191] L. Collins, et al., Breaking the time barrier in kelvin probe force microscopy: fast free force reconstruction using the G-mode platform, ACS Nano 11 (2017) 8717–8729.

[192] R. Giridharagopal, et al., Submicrosecond time resolution atomic force microscopy for probing nanoscale dynamics, Nano Lett. 12 (2012) 893–898.

[193] G. Gramse, A. Dols-Perez, M.A. Edwards, L. Fumagalli, G. Gomila, Nanoscale measurement of the dielectric constant of supported lipid bilayers in aqueous solutions with electrostatic force microscopy, Biophys. J. 104 (2013) 1257–1262.

[194] G. Gramse, A. Schönhals, F. Kienberger, Nanoscale dipole dynamics of protein membranes studied by broadband dielectric microscopy, Nanoscale 1764 (2019) 1647.

[195] Y.-H. Lu, et al., Infrared nanospectroscopy at the graphene–electrolyte interface, Nano Lett. 19 (2019) 5388–5393.

[196] S. Yang, et al., Nature of the electrical double layer on suspended graphene electrodes, J. Am. Chem. Soc. 144 (2022) 13327–13333.

[197] E. Strelcov, et al., Nanoscale mapping of the double layer potential at the graphene–electrolyte interface, Nano Lett. 20 (2020) 1336–1344.

[198] G. Gramse, M.A. Edwards, L. Fumagalli, G. Gomila, Theory of amplitude modulated electrostatic force microscopy for dielectric measurements in liquids at MHz frequencies, Nanotechnology 24 (2013).

[199] W. Trewby, K. Voïtchovsky, Nanoscale probing of local dielectric changes at the interface between solids and aqueous saline solutions, Faraday Discuss 246 (2023) 387–406.

[200] M.C. Biagi, et al., Nanoscale electric permittivity of single bacterial cells at gigahertz frequencies by scanning microwave microscopy, ACS Nano 10 (2016) 280–288.

[201] S. Grall, et al., Attoampere nanoelectrochemistry, Small 17 (2021): 2101253.

[202] R. Sivakumarasamy, et al., Selective layer-free blood serum ionogram based on ion-specific interactions with a nanotransistor, Nat. Mater. 17 (2018) 464–470.

[203] S.G. Lemay, et al., High-frequency nanocapacitor arrays: concept, recent developments, and outlook, Acc. Chem. Res. 49 (2016) 2355–2362.

[204] A.F. Nieuwenhuis, D.F. Duarte Sánchez, J.Z. Cui, S.G. Lemay, Stochastic electrical detection of single ion-gated semiconducting polymers, Adv. Mater. 35 (2023): 2307912.

[205] E. Gross, Challenges and opportunities in IR nanospectroscopy measurements of energy materials, Nano Res. 12 (2019) 2200–2210.

[206] C.L. Bentley, et al., Nanoscale electrochemical mapping, Anal. Chem. 91 (2019) 84–108.

[207] M.E. Snowden, et al., Scanning electrochemical cell microscopy: theory and experiment for quantitative high resolution spatially-resolved voltammetry and simultaneous ion-conductance measurements, Anal. Chem. 84 (2012) 2483–2491.

[208] S.M. Leitao, et al., Time-resolved scanning ion conductance microscopy for three-dimensional tracking of nanoscale cell surface dynamics, ACS Nano 15 (2021) 17613–17622.

[209] L. Zhou, Y. Gong, J. Hou, L.A. Baker, Quantitative visualization of nanoscale ion transport, Anal. Chem. 89 (2017) 13603–13609.

[210] G. Caniglia, G. Tezcan, G.N. Meloni, P.R. Unwin, C. Kranz, Probing and visualizing interfacial charge at surfaces in aqueous solution, Annu. Rev. Anal. Chem. 15 (2022) 247–267.

[211] P. Grochowski, J. Trylska, Continuum molecular electrostatics, salt effects, and counterion binding—a review of the Poisson–Boltzmann theory and its modifications, Biopolymers 89 (2008) 93–113.

[212] D. Bastos-González, L. Pérez-Fuentes, C. Drummond, J. Faraudo, Ions at interfaces: the central role of hydration and hydrophobicity, Curr. Opin. Colloid Interface Sci. 23 (2016) 19–28.

[213] D.C. Rapaport, The Art of Molecular Dynamics Simulation, Cambridge University Press, Cambridge, UK ; New York, NY, 2004.

[214] M.P. Allen, D.J. Tildesley, Computer Simulation of Liquids, Oxford University Press, Oxford, 2017.

[215] C. Tournassat, Y. Chapron, P. Leroy, M. Bizi, F. Boulahya, Comparison of molecular dynamics simulations with triple layer and modified Gouy–Chapman models in a 0.1M NaCl–montmorillonite system, J. Colloid Interface Sci. 339 (2009) 533–541.

[216] M. Rezaei, et al., Interfacial, electroviscous, and nonlinear dielectric effects on electrokinetics at highly charged surfaces, J. Phys. Chem. B 125 (2021) 4767–4778.

[217] I.C. Bourg, G. Sposito, Molecular dynamics simulations of the electrical double layer on smectite surfaces contacting concentrated mixed electrolyte (NaCl–CaCl2) solutions, J. Colloid Interface Sci. 360 (2011) 701–715.

[218] S.-J. Shin, et al., On the importance of the electric double layer structure in aqueous electrocatalysis, Nat. Commun. 13 (2022) 174.

[219] J.A. Kattirtzi, D.T. Limmer, A.P. Willard, Microscopic dynamics of charge separation at the aqueous electrochemical interface, Proc. Natl. Acad. Sci. U.S.A. 114 (2017) 13374–13379.

[220] M. Tavakol, et al., Disease-related metabolites affect protein–nanoparticle interactions, Nanoscale 10 (2018) 7108–7115.

[221] M.E. Tuckerman, Statistical Mechanics: Theory and Molecular Simulation, Oxford University Press, 2023, https://doi.org/10.1093/oso/9780198825562.001.0001.

[222] A. Pohorille, C. Chipot, Free Energy Calculations: Theory and Applications in Chemistry and Biology, Springer, Berlin, 2007.

[223] Y. Sugita, Y. Okamoto, Replica-exchange molecular dynamics method for protein folding, Chem. Phys. Lett. 314 (1999) 141–151.

[224] S. Grimme, Exploration of chemical compound, conformer, and reaction space with meta-dynamics simulations based on tight-binding quantum chemical calculations, J. Chem. Theor. Comput. 15 (2019) 2847–2862.

[225] D.J. Earl, M.W. Deem, Parallel tempering: theory, applications, and new perspectives, Phys. Chem. Chem. Phys. 7 (2005) 3910–3916.

[226] L. Rosso, P. Mináry, Z. Zhu, M.E. Tuckerman, On the use of the adiabatic molecular dynamics technique in the calculation of free energy profiles, J. Chem. Phys. 116 (2002) 4389–4402.

[227] H. Heinz, T.-J. Lin, R. Kishore Mishra, F.S. Emami, Thermodynamically consistent force fields for the assembly of inorganic, organic, and biological nanostructures: the INTERFACE force field, Langmuir 29 (2013) 1754–1765.

[228] L.B. Wright, P.M. Rodger, S. Corni, T.R. Walsh, GolP-CHARMM: first-principles based force fields for the interaction of proteins with Au(111) and Au(100), J. Chem. Theor. Comput. 9 (2013) 1616–1630.

[229] S.J.T. Brugman, et al., Calcite (104) surface–electrolyte structure: a 3D comparison of surface X-ray diffraction and simulations, J. Phys. Chem. C 124 (2020) 18564–18575.

[230] T. Zelovich, et al., Hydroxide ion diffusion in anion-exchange membranes at low hydration: insights from ab initio molecular dynamics, Chem. Mater. 31 (2019) 5778–5787.

[231] R.P. Misra, D. Blankschtein, Uncovering a universal molecular mechanism of salt ion adsorption at solid/water interfaces, Langmuir 37 (2021) 722–733.

[232] J. Huang, P.E.M. Lopes, B. Roux, A.D. MacKerell Jr., Recent advances in polarizable force fields for macromolecules: microsecond simulations of proteins using the classical drude oscillator model, J. Phys. Chem. Lett. 5 (2014) 3144–3150.

[233] S. Le Crom, C. Tournassat, J.-C. Robinet, V. Marry, Influence of water saturation level on electrical double layer properties in a clay mineral mesopore: a molecular dynamics study, J. Phys. Chem. C 126 (2022) 647–654.

[234] P. Raiteri, A. Schuitemaker, J.D. Gale, Ion pairing and multiple ion binding in calcium carbonate solutions based on a polarizable AMOEBA force field and ab initio molecular dynamics, J. Phys. Chem. B 124 (2020) 3568–3582.

[235] A. Warshel, M. Kato, A.V. Pisliakov, Polarizable force fields: history, test cases, and prospects, J. Chem. Theor. Comput. 3 (2007) 2034–2045.

[236] P.C.T. Souza, et al., Martini 3: a general purpose force field for coarse-grained molecular dynamics, Nat. Methods 18 (2021) 382–388.

[237] V. Rühle, C. Junghans, A. Lukyanov, K. Kremer, D. Andrienko, Versatile object-oriented Toolkit for coarse-graining applications, J. Chem. Theor. Comput. 5 (2009) 3211–3223.

[238] K.P. Santo, A.V. Neimark, Dissipative particle dynamics simulations in colloid and Interface science: a review, Adv. Colloid Interface Sci. 298 (2021): 102545.

[239] A. Zhmurov, R.I. Dima, Y. Kholodov, V. Barsegov, Sop-GPU: accelerating biomolecular simulations in the centisecond timescale using graphics processors, Proteins: Struct., Funct., Bioinf. 78 (2010) 2984–2999.

[240] S.J. Marrink, H.J. Risselada, S. Yefimov, D.P. Tieleman, A.H. De Vries, The MARTINI force field: coarse grained model for biomolecular simulations, J. Phys. Chem. B 111 (2007) 7812–7824.

[241] P. Vanýsek, Ionic conductivity and diffusion at infinite dilution, in: CRC Handbook of Chemistry and Physics, vols. 5–77, Taylor & Francis, Boca Raton, 2011, pp. 5–79.

[242] L. Cheng, P. Fenter, K.L. Nagy, M.L. Schlegel, N.C. Sturchio, Molecular-scale density oscillations in water adjacent to a mica surface, Phys. Rev. Lett. 87 (2001): 156103.

[243] F. Heberling, et al., Structure and reactivity of the calcite–water interface, J. Colloid Interface Sci. 354 (2011) 843–857.

[244] S. ben Jabrallah, et al., Electrolytes at interfaces: accessing the first nanometers using X-ray standing waves, Phys. Chem. Chem. Phys. 19 (2017) 167–174.

[245] P. Reichert, et al., Molecular scale structure and dynamics at an ionic liquid/electrode interface, Faraday Discuss 206 (2018) 141–157.

[246] H.-G. Steinrück, et al., The nanoscale structure of the electrolyte–metal oxide interface, Energy Environ. Sci. 11 (2018) 594–602.

[247] R.J. Alsop, R. Maria Schober, M.C. Rheinstädter, Swelling of phospholipid membranes by divalent metal ions depends on the location of the ions in the bilayers, Soft Matter 12 (2016) 6737–6748.

[248] W. Wang, R.Y. Park, A. Travesset, D. Vaknin, Ion-specific induced charges at aqueous soft interfaces, Phys. Rev. Lett. 106 (2011): 056102.

[249] J. Pittler, et al., Charge inversion at minute electrolyte concentrations, Phys. Rev. Lett. 97 (2006): 046102.

[250] J. Fitter, R.E. Lechner, N.A. Dencher, Interactions of hydration water and biological membranes studied by neutron scattering, J. Phys. Chem. B 103 (1999) 8036–8050.

[251] C. Park, P. Fenter, K. Nagy, N. Sturchio, Hydration and distribution of ions at the mica-water interface, Phys. Rev. Lett. 97 (2006): 016101.

[252] C. Park, P.A. Fenter, N.C. Sturchio, K.L. Nagy, Thermodynamics, interfacial structure, and pH hysteresis of Rb^{+} and Sr^{2+} adsorption at the muscovite (001)-solution interface, Langmuir 24 (2008) 13993–14004.

[253] S.S. Lee, P. Fenter, C. Park, N.C. Sturchio, K.L. Nagy, Hydrated cation speciation at the muscovite (001)-water interface, Langmuir 26 (2010) 16647–16651.

[254] S.S. Lee, P. Fenter, K.L. Nagy, N.C. Sturchio, Monovalent ion adsorption at the muscovite (001)–solution interface: relationships among ion coverage and speciation, interfacial water structure, and substrate relaxation, Langmuir 28 (2012) 8637–8650.

[255] I.C. Bourg, S.S. Lee, P. Fenter, C. Tournassat, Stern layer structure and energetics at mica–water interfaces, J. Phys. Chem. C 121 (2017) 9402–9412.

[256] R.R. Netz, H. Orland, Beyond Poisson-Boltzmann: fluctuation effects and correlation functions, Eur. Phys. J. E 1 (2000) 203–214.

[257] N.R. Agrawal, R. Wang, Electrostatic correlation induced ion condensation and charge inversion in multivalent electrolytes, J. Chem. Theor. Comput. 18 (2022) 6271–6280.

[258] A.A. Lee, C.S. Perez-Martinez, A.M. Smith, S. Perkin, Scaling analysis of the screening length in concentrated electrolytes, Phys. Rev. Lett. 119 (2017): 026002.

[259] D. Argyris, D.R. Cole, A. Striolo, Ion-specific effects under confinement: the role of interfacial water, ACS Nano 4 (2012) 2035–2042.

[260] C. Calero, J. Faraudo, D. Bastos-González, Interaction of monovalent ions with hydrophobic and hydrophilic colloids: charge inversion and ionic specificity, J. Am. Chem. Soc. 133 (2011) 15025–15035.

[261] H. Dongshuai, L. Zeyu, Z. Peng, D. Qingjun, Molecular structure and dynamics of an aqueous sodium chloride solution in nano-pores between portlandite surfaces: a molecular dynamics study, Phys. Chem. Chem. Phys. 18 (2016) 2059–2069.

[262] A. Serva, L. Scalfi, B. Rotenberg, M. Salanne, Effect of the metallicity on the capacitance of gold–aqueous sodium chloride interfaces, J. Chem. Phys. 155 (2021): 044703.

[263] Z. Li, V.G. Ruiz, M. Kanduč, J. Dzubiella, Highly heterogeneous polarization and solvation of gold nanoparticles in aqueous electrolytes, ACS Nano 15 (2021) 13155–13165.

[264] Y. Guo, et al., A molecular dynamics study on the effect of surfactant adsorption on heat transfer at a solid-liquid interface, Int. J. Heat Mass Tran. 135 (2019) 115–123.

[265] P. Zarzycki, Distance-dependent dielectric constant at the calcite/electrolyte interface: implication for surface complexation modeling, J. Colloid Interface Sci. 645 (2023) 752–764.

[266] J.-F. Olivieri, J.T. Hynes, D. Laage, Confined water's dielectric constant reduction is due to the surrounding low dielectric media and not to interfacial molecular ordering, J. Phys. Chem. Lett. 12 (2021) 4319–4326.

[267] A.P. Willard, S.K. Reed, P.A. Madden, D. Chandler, Water at an electrochemical interface—a simulation study, Faraday Discuss 141 (2009) 423–441.

[268] J. Lan, J. Hutter, M. Iannuzzi, First-principles simulations of an aqueous CO/Pt (111) interface, J. Phys. Chem. C 122 (2018) 24068–24076.

[269] J. Lan, V.V. Rybkin, M. Iannuzzi, Ionization of water as an effect of quantum delocalization at aqueous electrode interfaces, J. Phys. Chem. Lett. 11 (2020) 3724–3730.

[270] J. Cheng, M. Sprik, The electric double layer at a rutile TiO$_2$ water interface modelled using density functional theory based molecular dynamics simulation, J. Phys. Condens. Matter 26 (2014): 244108.

[271] D. Martin-Jimenez, R. Garcia, Identification of single adsorbed cations on mica–liquid interfaces by 3D force microscopy, J. Phys. Chem. Lett. 8 (2017) 5707–5711.

[272] J. Israelachvili, H. Wennerström, Role of hydration and water structure in biological and colloidal interactions, Nature 379 (1996) 219–225.

[273] J.N. Israelachvili, P.M. McGuiggan, Forces between surfaces in liquids, Science 241 (1988) 795–800.

[274] S.H. Khan, G. Matei, S. Patil, P.M. Hoffmann, Dynamic solidification in nanoconfined water films, Phys. Rev. Lett. 105 (2010): 106101.

[275] S.H. Khan, P.M. Hoffmann, Squeeze-out dynamics of nanoconfined water: a detailed nanomechanical study, Phys. Rev. E 92 (2015): 042403.

[276] T. Fukuma, M.J. Higgins, S.P. Jarvis, Direct imaging of individual intrinsic hydration layers on lipid bilayers at ångstrom resolution, Biophys. J. 92 (2007) 3603–3609.

[277] G. Bramley, M.-T. Nguyen, V.-A. Glezakou, R. Rousseau, C.-K. Skylaris, Reconciling work functions and adsorption enthalpies for implicit solvent models: a Pt (111)/water interface case study, J. Chem. Theor. Comput. 16 (2020) 2703–2715.

[278] S.M. Sarhangi, M.M. Waskasi, S.M. Hashemianzadeh, D.V. Matyushov, Effective dielectric constant of water at the interface with charged C60 fullerenes, J. Phys. Chem. B 123 (2019) 3135–3143.

[279] I. Ahmadabadi, A. Esfandiar, A. Hassanali, M.R. Ejtehadi, Structural and dynamical fingerprints of the anomalous dielectric properties of water under confinement, Phys. Rev. Mater. 5 (2021): 024008.

[280] V. Ballenegger, J.-P. Hansen, Dielectric permittivity profiles of confined polar fluids, J. Chem. Phys. 122 (2005): 114711.

[281] D.J. Bonthuis, S. Gekle, R.R. Netz, Profile of the static permittivity tensor of water at interfaces: consequences for capacitance, hydration interaction and ion adsorption, Langmuir 28 (2012) 7679–7694.

[282] J.-B. Le, Q.-Y. Fan, J.-Q. Li, J. Cheng, Molecular origin of negative component of Helmholtz capacitance at electrified Pt(111)/water interface, Sci. Adv. 6 (2020): eabb1219.

[283] M. Azimzadeh Sani, et al., Unexpectedly high capacitance of the metal nanoparticle/water interface: molecular-level insights into the electrical double layer, Angew. Chem. 134 (2022): e202112679.

[284] S.R. van Lin, K.K. Grotz, I. Siretanu, N. Schwierz, F. Mugele, Ion-specific and pH-dependent hydration of mica–electrolyte interfaces, Langmuir 35 (2019) 5737–5745.

[285] N. Schwierz, D. Horinek, U. Sivan, R.R. Netz, Reversed Hofmeister series—the rule rather than the exception, Curr. Opin. Colloid Interface Sci. 23 (2016) 10–18.

[286] N. Schwierz, D. Horinek, R.R. Netz, Specific ion binding to carboxylic surface groups and the ph dependence of the hofmeister series, Langmuir 31 (2015) 215–225.

[287] N. Kumar, M.P. Andersson, D. van den Ende, F. Mugele, I. Siretanu, Probing the surface charge on the basal planes of kaolinite particles with high-resolution atomic force microscopy, Langmuir 33 (2017) 14226–14237.

[288] B.A. Legg, K. Voïtchovsky, J.J. De Yoreo, Hydroxide films on mica form charge-stabilized microphases that circumvent nucleation barriers, Sci. Adv. 8 (2022): eabn7087.

[289] B.W. Hoogenboom, et al., Quantitative dynamic-mode scanning force microscopy in liquid, Appl. Phys. Lett. 88 (2006): 193109.

[290] E.T. Herruzo, H. Asakawa, T. Fukuma, R. Garcia, Three-dimensional quantitative force maps in liquid with 10 piconewton, angstrom and sub-minute resolutions, Nanoscale 5 (2013) 2678–2685.

[291] Y. Chen, et al., Nanoarchitecture factors of solid electrolyte interphase formation via 3D nano-rheology microscopy and surface force-distance spectroscopy, Nat. Commun. 14 (2023) 1321.

[292] S. Su, et al., Facet-dependent surface charge and hydration of semiconducting nanoparticles at variable pH, Adv. Mater. 33 (2021): 2106229.

[293] H. Söngen, et al., Chemical identification at the solid–liquid interface, Langmuir 33 (2017) 125–129.

[294] H. Söngen, et al., Resolving point defects in the hydration structure of calcite (10.4) with three-dimensional atomic force microscopy, Phys. Rev. Lett. 120 (2018): 116101.

[295] U.M. Ferber, G. Kaggwa, S.P. Jarvis, Direct imaging of salt effects on lipid bilayer ordering at sub-molecular resolution, Eur. Biophys. J. 40 (2011) 329–338.

[296] K.H. Sheikh, S.P. Jarvis, Crystalline hydration structure at the membrane-fluid interface of model lipid rafts indicates a highly reactive boundary region, J. Am. Chem. Soc. 133 (2011) 18296–18303.

[297] I. Siretanu, et al., Direct observation of ionic structure at solid-liquid interfaces: a deep look into the Stern Layer, Sci. Rep. 4 (2014) 4956.

[298] T. Fukuma, Y. Ueda, S. Yoshioka, H. Asakawa, Atomic-scale distribution of water molecules at the mica-water interface visualized by three-dimensional scanning force microscopy, Phys. Rev. Lett. 104 (2010): 016101.

[299] K. Miyazawa, M. Watkins, A.L. Shluger, T. Fukuma, Influence of ions on two-dimensional and three-dimensional atomic force microscopy at fluorite–water interfaces, Nanotechnology 28 (2017): 245701.

[300] T. Fukuma, et al., Mechanism of atomic force microscopy imaging of three-dimensional hydration structures at a solid-liquid interface, Phys. Rev. B 92 (2015): 155412.

[301] E. Nakouzi, et al., Moving beyond the solvent-tip approximation to determine site-specific variations of interfacial water structure through 3D force microscopy, J. Phys. Chem. C 125 (2021) 1282–1291.

[302] K. Miyata, Y. Kawagoe, N. Miyashita, T. Nakagawa, T. Fukuma, Atomic-scale structures and dynamics at the growing calcite step edge investigated by high-speed frequency modulation atomic force microscopy, Faraday Discuss 235 (2021) 551–561.

[303] K. Voïtchovsky, High-resolution AFM in liquid: what about the tip? Nanotechnology 26 (2015): 100501.

[304] G.B. Kaggwa, P.C. Nalam, J.I. Kilpatrick, N.D. Spencer, S.P. Jarvis, Impact of hydrophilic/hydrophobic surface chemistry on hydration forces in the absence of confinement, Langmuir 28 (2012) 6589–6594.

[305] K. Voïtchovsky, Anharmonicity, solvation forces, and resolution in atomic force microscopy at the solid-liquid interface, Phys. Rev. E 88 (2013): 022407.

[306] S. Benaglia, et al., Tip charge dependence of three-dimensional AFM mapping of concentrated ionic solutions, Phys. Rev. Lett. 127 (2021): 196101.

[307] J. Tracey, et al., Understanding 2D atomic resolution imaging of the calcite surface in water by frequency modulation atomic force microscopy, Nanotechnology 27 (2016): 415709.

[308] B. Reischl, M. Watkins, A.S. Foster, Free energy approaches for modeling atomic force microscopy in liquids, J. Chem. Theor. Comput. 9 (2013) 600–608.

[309] M. Watkins, B. Reischl, A simple approximation for forces exerted on an AFM tip in liquid, J. Chem. Phys. 138 (2013): 154703.

[310] M.R. Uhlig, S. Benaglia, R. Thakkar, J. Comer, R. Garcia, Atomically resolved interfacial water structures on crystalline hydrophilic and hydrophobic surfaces, Nanoscale 13 (2021) 5275–5283.

[311] Y.S. Ranawat, Y.M. Jaques, A.S. Foster, Generalised deep-learning workflow for the prediction of hydration layers over surfaces, J. Mol. Liq. 367 (2022): 120571.

[312] Y.S. Ranawat, Y.M. Jaques, A.S. Foster, Predicting hydration layers on surfaces using deep learning, Nanoscale Adv. 3 (2021) 3447–3453.

[313] S. Dewan, et al., Structure of water at charged interfaces: a molecular dynamics study, Langmuir 30 (2014) 8056–8065.

[314] A. Rojano, A. Córdoba, J.H. Walther, H.A. Zambrano, Effect of charge inversion on nanoconfined flow of multivalent ionic solutions, Phys. Chem. Chem. Phys. 24 (2022) 4935–4943.

[315] S.K. Natarajan, J. Behler, Neural network molecular dynamics simulations of solid–liquid interfaces: water at low-index copper surfaces, Phys. Chem. Chem. Phys. 18 (2016) 28704–28725.

[316] R. Nadler, J.F. Sanz, First-principles molecular dynamics simulations of the H2O/Cu(111) interface, J. Mol. Model. 18 (2012) 2433–2442.

[317] S. Izvekov, A. Mazzolo, K. VanOpdorp, G.A. Voth, *Ab initio* molecular dynamics simulation of the Cu(110)–water interface, J. Chem. Phys. 114 (2001) 3248–3257.

[318] A.P. Willard, D.T. Limmer, P.A. Madden, D. Chandler, Characterizing heterogeneous dynamics at hydrated electrode surfaces, J. Chem. Phys. 138 (2013): 184702.

[319] D.T. Limmer, A.P. Willard, P. Madden, D. Chandler, Hydration of metal surfaces can be dynamically heterogeneous and hydrophobic, Proc. Natl. Acad. Sci. U.S.A. 110 (2013) 4200–4205.

[320] A. Mendhe, H.S. Panda, A review on electrolytes for supercapacitor device, Discov. Mater. 3 (2023) 29.

[321] T. Ando, High-speed atomic force microscopy and its future prospects, Biophys. Rev. 10 (2018) 285–292.

[322] P. Klapetek, et al., Large area high-speed metrology SPM system, Nanotechnology 26 (2015): 065501.

[323] S.S. Lee, F. Heberling, N.C. Sturchio, P.J. Eng, P. Fenter, Surface charge of the calcite (104) terrace measured by $Rb+$ adsorption in aqueous solutions using resonant anomalous X-ray reflectivity, J. Phys. Chem. C 120 (2016) 15216–15223.

[324] S.S. Lee, P. Fenter, K.L. Nagy, N.C. Sturchio, Changes in adsorption free energy and speciation during competitive adsorption between monovalent cations at the muscovite (001)-water interface, Geochem. Cosmochim. Acta 123 (2013) 416–426.

[325] W.H.H. Woodward, Broadband dielectric spectroscopy—a practical guide, in: W. H.H. Woodward (Ed.), ACS Symposium Series, vol. 1375, American Chemical Society, Washington, DC, 2021, pp. 3–59.

[326] G. Gramse, A. Dols-Pérez, M.A. Edwards, L. Fumagalli, G. Gomila, Quantitative dielectric measurements of biomembranes and oxides in electrolyte solutions at high frequencies, Biophys. J. 106 (2014) 512a.

[327] E. Spohr, Molecular dynamics simulations of water and ion dynamics in the electrochemical double layer, Solid State Ionics 150 (2002) 1–12.

[328] D.J. Evans, G. Morriss, Statistical Mechanics of Nonequilibrium Liquids, Cambridge University Press, 2008, https://doi.org/10.1017/CBO9780511535307.

[329] D. Frenkel, B. Smit, Understanding Molecular Simulation, Academic Press, San Diego, 2002, https://doi.org/10.1016/B978-012267351-1/50000-6.

[330] R.P. Feynman, There's plenty of room at the bottom, Eng. Sci. 23 (1959).